Inorganic Chemistry

Article

pubs.acs.org/IC

Structural and Spectroscopic Trends in a Series of Half-Sandwich Scorpionate Complexes

Shengwen Liang,[†] Haoshuang Wang,[†] Tapash Deb,[†] Jeffrey L. Petersen,[‡] Gordon T. Yee,[§] and Michael P. Jensen*,[†]

[†]Department of Chemistry and Biochemistry, Ohio University, Athens, Ohio 45701, United States

[‡]C. Eugene Bennett Department of Chemistry, West Virginia University, Morgantown, West Virginia 26506, United States

[§]Department of Chemistry, Virginia Polytechnic Institute and State University, Blacksburg, Virginia 24061, United States

Supporting Information

ABSTRACT: Fifteen half-sandwich scorpionate complexes $[(L)M(NCMe)_3](BF_4)_n$ (L = tris(3,5-dimethylpyrazol-1-yl)methane, $Tpm^{Me,Me}$, n = 2, $\mathbf{1}^M$, M = Mn, Fe, Co, Ni; L = tris(3-phenylpyrazol-1-yl)methane, Tpm^{Ph}, n = 2, $\mathbf{2}^M$, M = Mn, Fe, Co, Ni; L = hydrotris(3,5-dimethylpyrazol-1-yl)borate, $[Tp^{Me,Me}]^-$, n = 1, $\mathbf{3}^M$, M = Fe, Co, Ni; L = hydrotris(3-phenyl-5-methylpyrazol-1-yl)borate, $[Tp^{Ph,Me}]^-$, n = 1, $\mathbf{4}^M$, M = Mn, Fe, Co, Ni) were prepared by addition of the tripodal ligands to solvated $[M(NCMe)_x]^{2+}$ (M = Mn, x = 4; M = Fe, Co, Ni, x = 6) precursor complexes. The product complexes were characterized by ^{1}H NMR (except M = Mn), UV−vis−NIR, and FTIR spectroscopy. The structures of $\mathbf{2}^{Mn}$, $\mathbf{2}^{Ni}$, $\mathbf{3}^{Fe}$, $\mathbf{3}^{Co}$, and $\mathbf{4}^{Fe}$ were determined by X-ray crystallography. The data were consistent with complexes of high-spin divalent metal ions in idealized piano-stool geometries in all cases. Consequent lability of the acetonitrile ligands will enable use of these complexes as synthetic precursors and as catalysts. Comparison to previously reported structures of $\mathbf{1}^{Fe}$, $\mathbf{1}^{Co}$, $\mathbf{2}^{Fe}$, and $\mathbf{2}^{Co}$, the triflate salt analogues of $\mathbf{4}^{Co}$ and $\mathbf{4}^{Ni}$, as well as related sandwich complexes (e.g., $[(Tp^{Me,Me})_2M]$) and solvated metal dications $[M(NCMe)_6]^{2+}$ reveals numerous trends in M−N bond lengths. Primary among these are the Irving−Williams series, with significant structural effects also arising from ligand charge and sterics. Systematic trends in spectroscopic data were also observed which further elucidate these issues.

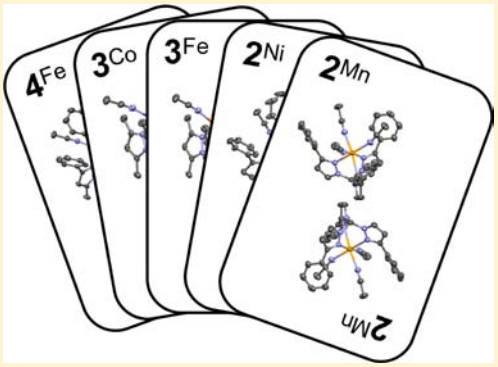

1. INTRODUCTION

Hydrotris(pyrazol-1-yl)borates (i.e., $HB\{pz\}_3^-$, Tp)[1−3] and tris(pyrazol-1-yl)methanes (i.e., $HC(pz)_3$, Tpm)[4−6] are tridentate face-capping ligands, formally isolobal to the cyclopentadienyl anion ($C_5H_5^-$, Cp), that have been extensively utilized in bioinorganic and organometallic chemistry. A wide variety of half-sandwich complexes can be supported, which have been exploited as enzyme active site models and as functional catalysts. For example, Tp-supported copper complexes (i.e., $[Tp^{Br3}Cu(NCMe)]$) have been used as nitrene transfer catalysts, promoting olefin aziridination and amination of aliphatic and aromatic C−H bonds.[7] Analogous catalysis was also reported using $[Tpm^RCu(NCMe)]BF_4$ in ionic liquids.[8]

Despite the success of copper complexes as catalysts in nitrene transfer reactions, the use of scorpionate complexes of other late 3d metal ions in such catalysis has not been investigated, although several pseudo-tetrahedral imido complexes have been characterized for Fe^{III},[9−11] Fe^{IV},[10,11] and Co^{III}.[12−14] Analogous to the solvated pseudotetrahedral copper catalysts just described, we prepared a series of pseudo-octahedral half-sandwich scorpionate complexes of divalent metal ions (i.e., Mn^{II}, Fe^{II}, Co^{II}, Ni^{II}). These complexes exhibit high-spin ground states, and the resulting occupation of dσ* orbitals (i.e., e_g under ideal O_h symmetry) induces lability in the acetonitrile coligands. This renders the complexes potentially useful both as synthetic reagents and as catalysts; indeed, we have examined the complexes as catalysts in nitrene transfer reactivity, akin to the copper analogues,[7,8] and these results are reported elsewhere.[15] In the present work, we report synthesis and characterization of the complexes, which revealed significant metal- and ligand-dependent structural and spectroscopic trends that require separate consideration.

The complexes reported herein include $[(L)M(NCMe)_3](BF_4)_n$ (Scheme 1: L = tris(3,5-dimethylpyrazol-1-yl)methane, $Tpm^{Me,Me}$, n = 2, $\mathbf{1}^M$, M = Mn, Fe, Co, Ni; L = tris(3-phenylpyrazol-1-yl)methane, Tpm^{Ph}, n = 2, $\mathbf{2}^M$, M = Mn, Fe, Co, Ni; L = hydrotris(3,5-dimethylpyrazol-1-yl)borate, $[Tp^{Me,Me}]^-$, n = 1, $\mathbf{3}^M$, M = Fe, Co, Ni; L = hydrotris(3-phenyl-5-methylpyrazol-1-yl)borate, $[Tp^{Ph,Me}]^-$, n = 1, $\mathbf{4}^M$, M = Mn, Fe, Co, Ni). The attempted synthesis of $\mathbf{3}^{Mn}$ yielded the known sandwich complex $[(Tp^{Me,Me})_2Mn]$.[16] The fifteen other complexes were obtained in 62−98% yields by displacement of acetonitrile ligands by tripodal scorpionate ligands from

Received: June 29, 2012
Published: November 19, 2012

Scheme 1

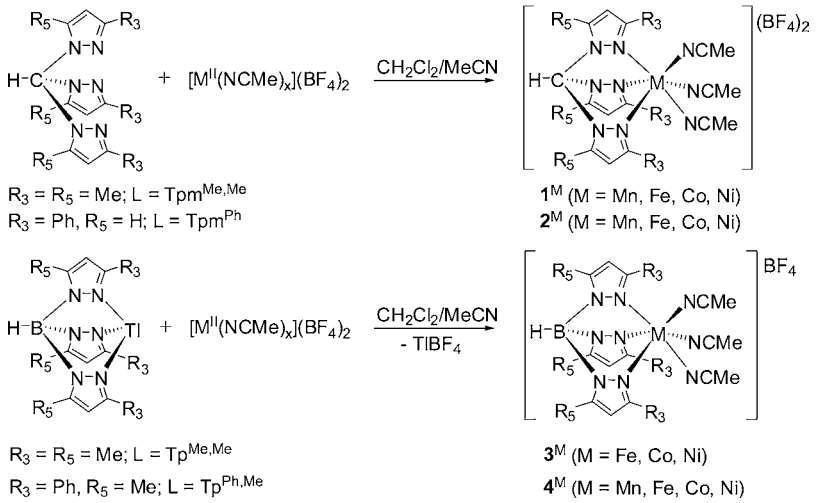

previously characterized precursor complexes $[M(NCMe)_x](BF_4)_2$ (M = Mn, x = 4; M = Fe, Co, Ni, x = 6).[17] The structures and IR spectra of $[Tpm^{Me,Me}M(NCMe)_3](BF_4)_2$ (i.e., $\mathbf{1}^M$, M = Fe, Co),[18] $[Tpm^{Ph}M(NCMe)_3](BF_4)_2$ ($\mathbf{2}^M$, M = Fe, Co),[18] and $[Tp^{Ph,Me}M(NCMe)_3]OTf$ (M = Co, Ni)[19] were reported previously. We have added structural characterization of five new complexes ($\mathbf{2}^{Mn}$, $\mathbf{2}^{Ni}$, $\mathbf{3}^{Fe}$, $\mathbf{3}^{Co}$ and $\mathbf{4}^{Fe}$) and have fully characterized all the complexes by ^{1}H NMR (except $\mathbf{1}^{Mn}$–$\mathbf{4}^{Mn}$), UV–vis–NIR and FTIR spectroscopy. For comparative purposes, we also report the X-ray structure of $[(Tp^{Ph,Me})_2Fe]$.

While isoelectronic Tp- and Tpm-supported metal centers are expected to exhibit comparable structures and analogous reactivities, the greater positive charge on the dicationic Tpm complexes may enhance Lewis acidity and promote electrophilic reaction mechanisms. Therefore, the Tp- and Tpm-supported complexes may exhibit different reactivities. A further consideration is the ability to manipulate steric and electronic donor properties of the ligands by incorporating substituents on the pyrazole rings.[1−6] Structural and spectroscopic data obtained in the present work revealed significant trends in the half-sandwich complexes that illuminate these issues.

2. EXPERIMENTAL SECTION

General Procedures. All manipulations were carried out under an inert atmosphere, either in an argon-filled glovebox (MBraun Unilab) or under nitrogen using Schlenk techniques. The solvated metal salts, $[M(NCMe)_x](BF_4)_2$ (M = Mn, x = 4; M = Fe, Co, Ni, x = 6) were obtained by $NOBF_4$ oxidation of metal powders in CH_3CN, as previously described;[17] the metal powders were purchased from Aldrich and used without further purification. Tris(3,5-dimethylpyrazol-1-yl)methane ($Tpm^{Me,Me}$)[20] and tris(3-phenylpyrazol-1-yl)-methane (Tpm^{Ph})[21] were prepared by literature syntheses. Thallium salts of hydrotris(pyrazol-1-yl)borates ($TlTp^{R,Me}$; R = Me, Ph) were obtained as previously described [***Caution!*** *Thallium salts are extremely toxic, and must be properly handled and disposed.*].[22] Dichloromethane (CH_2Cl_2) and acetonitrile (CH_3CN) were degassed and distilled from calcium hydride (CaH_2) under nitrogen. Diethyl ether (Et_2O) was degassed and distilled over sodium/benzophenone.

^{1}H NMR data were recorded on a Varian Unity (500 MHz) spectrometer and processed using the MestReNova software suite (Mestrelab Research, Santiago de Compostela, Spain); spectra were referenced internally to free CH_3CN (1.96 ppm).[23] CD_3CN was distilled under vacuum from CaH_2 and degassed by the freeze–pump–thaw method prior to use. Magnetic moments were determined in CD_3CN solutions at 295 K by the Evans NMR method.[24] FTIR spectra were recorded from KBr pellets on a Thermo-Electron Nicolet 380 spectrophotometer. UV–vis–NIR spectra were recorded on an Agilent HP-8453 diode-array spectrophotometer. Elemental analyses were performed by Atlantic Microlabs, Inc. (Norcross, GA); as noted previously,[18,19] data typically reflect partial or complete loss of coordinated acetonitrile ligands. TGA data were obtained using a TA Instruments SDT Q600 instrument. Solid state magnetic susceptibility data were collected from 5 to 300 K at 0.1 T on an MPMS 7T SQUID magnetometer; Pascal's constants were used to estimate diamagnetic corrections.

Preparation of $[Tpm^{Me,Me}Mn(NCMe)_3](BF_4)_2$ ($\mathbf{1}^{Mn}$). To a solution of $[Mn(NCMe)_4](BF_4)_2$ (196.4 mg, 0.5 mmol) in CH_3CN (20 mL) was added dropwise a solution of $Tpm^{Me,Me}$ (149.2 mg, 0.5 mmol) in CH_2Cl_2 (20 mL) at room temperature. The mixture was stirred overnight, and solvents were removed under vacuum to yield a light yellow solid residue. The residue was extracted into CH_3CN (10 mL), then solvent was removed after stirring 10 m. Colorless crystals of $\mathbf{1}^{Mn}$ were obtained by vapor diffusion of diethyl ether into a concentrated CH_3CN solution at room temperature. Yield: 291 mg (0.45 mmol, 90%). Anal. Calcd (found) for $C_{22}H_{33}B_2F_8MnN_9O$, $\mathbf{1}^{Mn}\cdot H_2O$: C, 39.55 (40.04); H, 4.98 (4.81); N, 18.87 (18.97). μ_{eff} = 5.90 μ_B. FTIR (KBr, cm^{-1}): 2313, ν(C≡N); 2281, ν(C≡N).

Preparation of $[Tpm^{Me,Me}Fe(NCMe)_3](BF_4)_2$ ($\mathbf{1}^{Fe}$).[18] The previously reported light yellow complex salt was prepared as described for $\mathbf{1}^{Mn}$ from $[Fe(NCMe)_6](BF_4)_2$ (237.9 mg, 0.5 mmol) and $Tpm^{Me,Me}$ (149.2 mg, 0.5 mmol). Yield: 321 mg (0.49 mmol, 98%). ^{1}H NMR (CD_3CN, 295 K; δ, ppm): 55.9 (3H, 4-pz); 46.5 (9H, 3-Me); 14.9 (9H, 5-Me); −58.4 (1H, C–H). μ_{eff} = 5.87 μ_B. UV–vis (CH_3CN, λ_{max}, nm; ε, M^{-1} cm^{-1}): 863 (6.1). FTIR (KBr, cm^{-1}): 2313, ν(C≡N); 2283, ν (C≡N).

Preparation of $[Tpm^{Me,Me}Co(NCMe)_3](BF_4)_2$ ($\mathbf{1}^{Co}$).[18] The previously reported orange complex salt was prepared as described for $\mathbf{1}^{Mn}$ from $[Co(NCMe)_6](BF_4)_2$ (239.4 mg, 0.5 mmol) and $Tpm^{Me,Me}$ (149.2 mg, 0.5 mmol). Yield: 314 mg (0.48 mmol, 96%). ^{1}H NMR (CD_3CN, 295 K; δ, ppm): 106.5 (1H, C–H); 55.8 (3H, 4-pz); 44.0 (9H, 5-Me); −70.2 (9H, 3-Me). μ_{eff} = 4.99 μ_B. UV–vis (CH_3CN, λ_{max}, nm; ε, M^{-1} cm^{-1}): 467 (32.6), 516 (16.1, sh), 972 (2.8). FTIR (KBr, cm^{-1}): 2314, ν(C≡N); 2287, ν(C≡N).

Preparation of $[Tpm^{Me,Me}Ni(NCMe)_3](BF_4)_2$ ($\mathbf{1}^{Ni}$). The blue-purple complex salt was prepared as for $\mathbf{1}^{Mn}$ from $[Ni(NCMe)_6](BF_4)_2$ (239.3 mg, 0.5 mmol) and $Tpm^{Me,Me}$ (149.2 mg, 0.5 mmol). Yield: 318 mg (0.49 mmol, 97%). Anal. Calcd (found) for $C_{20}H_{28}B_2F_8N_8Ni$, $\mathbf{1}^{Ni}$–NCMe: C, 39.20 (38.08); H, 4.61 (4.68); N, 18.29 (18.24). ^{1}H NMR (CD_3CN, 295 K; δ, ppm): 58.5 (3H, 4-pz); −3.0 (9H, 5-Me); −9.0 (10H, 3-Me + C–H). μ_{eff} = 3.14 μ_B. UV–vis

dx.doi.org/10.1021/ic301409s | Inorg. Chem. 2012, 51, 12707−12719

(CH_3CN, λ_{max}, nm; ε, M^{-1} cm^{-1}): 581 (16.6), 743 (3.1), 925 (5.5). FTIR (KBr, cm^{-1}): 2319, ν(C≡N); 2291, ν(C≡N).

Preparation of [Tpm^{Ph}Mn(NCMe)$_3$](BF$_4$)$_2$ (2^{Mn}). The light yellow complex salt was prepared as for **1**^{Mn} from [Mn(NCMe)$_4$](BF$_4$)$_2$ (196.4 mg, 0.5 mmol) and Tpm^{Ph} (221.3 mg, 0.5 mmol). Yield: 315 mg (0.40 mmol, 79%). Anal. Calcd (found) for $C_{34}H_{33}B_2F_8MnN_9O$, **2**^{Mn}·H_2O: C, 50.28 (50.55); H, 4.10 (3.88); N, 15.52 (15.51). μ_{eff} = 5.94 μ_B. FTIR (KBr, cm^{-1}): 2308, ν(C≡N); 2280, ν(C≡N).

Preparation of [Tpm^{Ph}Fe(NCMe)$_3$](BF$_4$)$_2$·MeCN (2^{Fe}·MeCN).[18] The previously reported light yellow complex salt was prepared as for **1**^{Mn} from [Fe(NCMe)$_6$](BF$_4$)$_2$ (237.9 mg, 0.5 mmol) and Tpm^{Ph} (221.3 mg, 0.5 mmol). Yield: 390 mg (0.47 mmol, 93%). ^{1}H NMR (CD_3CN, 295 K; δ, ppm): 47.6 (3H, 4-pz); 27.4 (6H, 3-*o*-Ph); 12.8 (6H, 3-*m*-Ph); −4.5 (3H, 5-pz); −53.4 (1H, C−H). μ_{eff} = 5.75 μ_B. UV−vis (CH_3CN, λ_{max}, nm; ε, M^{-1} cm^{-1}): 905 (10.6). FTIR (KBr, cm^{-1}): 2308, ν(C≡N); 2282, ν(C≡N).

Preparation of [Tpm^{Ph}Co(NCMe)$_3$](BF$_4$)$_2$·MeCN (2^{Co}·MeCN).[18] The previously reported orange complex salt was prepared as for **1**^{Mn} from [Co(NCMe)$_6$](BF$_4$)$_2$ (239.4 mg, 0.5 mmol) and Tpm^{Ph} (221.3 mg, 0.5 mmol). Yield: 387 mg (0.46 mmol, 92%). ^{1}H NMR (CD_3CN, 295 K; δ, ppm): 110.8 (1H, C−H); 75.3 (3H, 5-pz); 47.3 (3H, 4-pz); 1.1 (3H, 3-*p*-Ph); −4.4 (6H, 3-*m*-Ph); −57.3 (6H, 3-*o*-Ph). μ_{eff} = 4.96 μ_B. UV−vis (CH_3CN, λ_{max}, nm; ε, M^{-1} cm^{-1}): 470 (40.9), 512 (31.4, sh), 992 (2.8). FTIR (KBr, cm^{-1}): 2315, ν(C≡N); 2290, ν(C≡N).

Preparation of [Tpm^{Ph}Ni(NCMe)$_3$](BF$_4$)$_2$·MeCN (2^{Ni}·MeCN). The blue-purple complex salt was prepared as for **1**^{Mn} from [Ni(NCMe)$_6$](BF$_4$)$_2$ (239.3 mg, 0.5 mmol) and Tpm^{Ph} (221.3 mg, 0.5 mmol). Yield: 356 mg (0.42 mmol, 85%). Anal. Calcd (found) for $C_{36}H_{36}B_2F_8NiN_{10}O$, **2**^{Ni}·NCMe·$H_2O$: C, 50.45 (50.32); H, 4.23 (4.01); N, 16.34 (16.18). ^{1}H NMR (CD_3CN, 295 K; δ, ppm): 49.6 (3H, 4-pz); 40.2 (3H, 5-pz); −7.3 (1H, C−H). μ_{eff} = 3.01 μ_B. UV−vis (CH_3CN, λ_{max}, nm; ε, M^{-1} cm^{-1}): 588 (24.4), 972 (5.9). FTIR (KBr, cm^{-1}): 2318, ν(C≡N); 2290, ν(C≡N).

Attempted preparation of [Tp^{Me,Me}Mn(NCMe)$_3$]BF$_4$ (3^{Mn}). Various attempts to prepare **3**^{Mn} were not successful; instead, the previously reported sandwich complex [(Tp^{Me,Me})$_2$Mn] was obtained.[16] Anal. Calcd (found) for $C_{30}H_{44}B_2MnN_{12}$: C, 55.49 (55.56); H, 6.83 (6.78); N, 25.89 (26.05).

Preparation of [Tp^{Me,Me}Fe(NCMe)$_3$]BF$_4$·^{1}/$_2$MeCN (3^{Fe}·^{1}/$_2$MeCN). To a solution of [Fe(NCMe)$_6$](BF$_4$)$_2$ (237.9 mg, 0.5 mmol) in CH_3CN (20 mL) was added dropwise a solution of TlTp^{Me,Me} (250.8 mg, 0.5 mmol) in CH_2Cl_2 (20 mL) at room temperature. The mixture was allowed to stir overnight, and the solvents were removed under vacuum. The resulting orange solid was extracted into CH_2Cl_2 (20 mL). The extracts were filtered and evaporated to yield an orange solid. Light orange crystals were obtained by vapor diffusion of diethyl ether into concentrated CH_3CN solution of **3**^{Fe} at room temperature. Yield: 196 mg (0.34 mmol, 67%). Anal. Calcd (found) for $C_{15}H_{22}B_2F_4FeN_6$, **3**^{Fe}−3NCMe: C, 40.96 (40.70); H, 5.04 (5.75); N, 19.11 (18.71). ^{1}H NMR (CD_3CN, 295 K; δ, ppm): 58.4 (3H, 4-pz); 48.4 (9H, 3-Me); 16.8 (9H, 5-Me); −60.6 (1H, B−H). μ_{eff} = 5.62 μ_B. UV−vis (CH_3CN, λ_{max}, nm; ε, M^{-1} cm^{-1}): 478 (93.0), 830 (9.5). FTIR (KBr, cm^{-1}): 2540, ν(B−H); 2311, ν(C≡N); 2278, ν(C≡N).

Preparation of [Tp^{Me,Me}Co(NCMe)$_3$]BF$_4$·^{1}/$_2$MeCN (3^{Co}·^{1}/$_2$MeCN). The orange complex salt was prepared as for **3**^{Fe} from [Co(NCMe)$_6$](BF$_4$)$_2$ (239.4 mg, 0.5 mmol) and TlTp^{Me,Me} (250.8 mg, 0.5 mmol). Yield: 184 mg (0.31 mmol, 63%). Anal. Calcd (found) for $C_{15}H_{23}B_2CoF_4N_6O_{0.5}$, **3**^{Co}·^{1}/$_2$$H_2O$−3NCMe: C, 39.86 (39.57); H, 5.13 (5.40); N, 18.60 (18.72). ^{1}H NMR (CD_3CN, 295 K; δ, ppm): 77.9 (1H, B−H); 56.9 (3H, 4-pz); 39.5 (9H, 5-Me); −56.1 (9H, 3-Me). μ_{eff} = 4.80 μ_B. UV−vis (CH_3CN, λ_{max}, nm; ε, M^{-1} cm^{-1}): 483 (45.7), 503 (45.4, sh), 527 (46.9, sh), 581 (40.3), 621 (29.6, sh), 1021 (10.8). FTIR (KBr, cm^{-1}): 2526, ν(B−H); 2303, ν(C≡N); 2277, ν(C≡N).

Preparation of [Tp^{Me,Me}Ni(NCMe)$_3$]BF$_4$ (3^{Ni}). The blue complex salt was prepared as for **3**^{Fe} from [Ni(NCMe)$_6$](BF$_4$)$_2$ (239.3 mg, 0.5 mmol) and TlTp^{Me,Me} (250.8 mg, 0.5 mmol). Yield: 175 mg (0.31 mmol, 62%). Anal. Calcd (found) for $C_{17}H_{26}B_2F_4N_7NiO_{0.5}$, **3**^{Ni}·^{1}/$_2$$H_2O$−2NCMe: C, 41.44 (42.00); H, 5.32 (5.72); N, 19.90 (19.38). ^{1}H NMR (CD_3CN, 295 K; δ, ppm): 63.2 (3H, 4-pz); −2.3 (9H, 5-Me); −7.7 (9H, 3-Me); −12.0 (1H, B−H). μ_{eff} = 2.81 μ_B. UV−vis (CH_3CN, λ_{max}, nm; ε, M^{-1} cm^{-1}): 375 (30.0), 597 (21.3), 757 (4.0), 943 (10.6). FTIR (KBr, cm^{-1}): 2523, ν(B−H); 2323, ν(C≡N); 2298, ν(C≡N).

Preparation of [Tp^{Ph,Me}Mn(NCMe)$_3$]BF$_4$ (4^{Mn}). The colorless complex salt was prepared as for **3**^{Fe} from [Mn(NCMe)$_4$](BF$_4$)$_2$ (196.4 mg, 0.5 mmol) and TlTp^{Ph,Me} (343.9 mg, 0.5 mmol). Yield: 286 mg (0.38 mmol, 76%). Anal. Calcd (found) for $C_{32}H_{33}B_2F_4MnN_7O$, **4**^{Mn}·H_2O−2NCMe: C, 56.17 (56.48); H, 4.86 (4.94); N, 14.33 (13.86). μ_{eff} = 5.90 μ_B. FTIR (KBr, cm^{-1}): 2550, ν(B−H); 2308, ν(C≡N); 2280, ν(C≡N).

Preparation of [Tp^{Ph,Me}Fe(NCMe)$_3$]BF$_4$·^{1}/$_2$MeCN (4^{Fe}·^{1}/$_2$MeCN). The colorless complex salt was prepared as for **3**^{Fe} from [Fe(NCMe)$_6$](BF$_4$)$_2$ (237.9 mg, 0.5 mmol) and TlTp^{Ph,Me} (343.9 mg, 0.5 mmol). Yield: 323 mg (0.42 mmol, 84%). Anal. Calcd (found) for $C_{32}H_{33}B_2F_4FeN_7O$, **4**^{Fe}·H_2O−2NCMe: C, 56.10 (56.12); H, 4.85 (4.94); N, 14.31 (14.40). ^{1}H NMR (CD_3CN, 295 K; δ, ppm): 55.4 (3H, 4-pz); 29.6 (6H, 3-*o*-Ph); 21.1 (9H, 5-Me); 10.9 (6H, 3-*m*-Ph); 6.8 (3H, 3-*p*-Ph); −56.3 (1H, B−H). μ_{eff} = 5.27 μ_B. UV−vis (CH_3CN, λ_{max}, nm; ε, M^{-1} cm^{-1}): 839 (5.4). FTIR (KBr, cm^{-1}): 2548, ν(B−H); 2310, ν(C≡N); 2281, ν(C≡N).

Preparation of [Tp^{Ph,Me}Co(NCMe)$_3$]BF$_4$ (4^{Co}). The orange complex, previously reported as the triflate salt,[19] was prepared as for **3**^{Fe} from [Co(NCMe)$_6$](BF$_4$)$_2$ (239.4 mg, 0.5 mmol) and TlTp^{Ph,Me} (343.9 mg, 0.5 mmol). Yield: 300 mg (0.40 mmol, 80%). Anal. Calcd (found) for $C_{32}H_{37}B_2CoF_4N_7O_3$, **4**^{Co}·$3H_2O$−2NCMe: C, 53.07 (53.59); H, 5.15 (4.91); N, 13.54 (13.55). ^{1}H NMR (CD_3CN, 295 K; δ, ppm): 69.5 (1H, B−H); 57.1 (3H, 4-pz); 42.1 (9H, 5-Me); 5.2 (3H, 3-*p*-Ph); 2.7 (6H, 3-*m*-Ph); −37.3 (6H, 3-*o*-Ph). μ_{eff} = 4.82 μ_B. UV−vis (CH_3CN, λ_{max}, nm; ε, M^{-1} cm^{-1}): 468 (38.4), 519 (48.4), 551 (42.5), 989 (6.7). FTIR (KBr, cm^{-1}): 2547, ν(B−H); 2314, ν(C≡N); 2287, ν(C≡N).

Preparation of [Tp^{Ph,Me}Ni(NCMe)$_3$]BF$_4$ (4^{Ni}). The blue complex, previously reported as the triflate salt,[19] was prepared as for **3**^{Fe} from [Ni(NCMe)$_6$](BF$_4$)$_2$ (239.3 mg, 0.5 mmol) and TlTp^{Ph,Me} (343.9 mg, 0.5 mmol). Yield: 240 mg (0.32 mmol, 64%). Anal. Calcd (found) for $C_{32}H_{35}B_2F_4N_7NiO_2$, **4**^{Ni}·$2H_2O$−2NCMe: C, 54.44 (54.78); H, 5.00 (4.86); N, 13.89 (14.36). ^{1}H NMR (CD_3CN, 295 K; δ, ppm): 63.8 (3H, 4-pz); 8.0 (6H, 3-*m*-Ph); 7.0 (9H, 3-*o*-Ph + 3-*p*-Ph); 1.6 (9H, 5-Me); −10.8 (1H, B−H). μ_{eff} = 2.94 μ_B. UV−vis (CH_3CN, λ_{max}, nm; ε, M^{-1} cm^{-1}): 605 (21.5), 757 (6.1), 839 (8.1). FTIR (KBr, cm^{-1}): 2546, ν(B−H); 2316, ν(C≡N); 2290, ν(C≡N).

Preparation of [(Tp^{Ph,Me})$_2$Fe]. To a solution of [Tp^{Ph,Me}Fe(CH$_3$CN)$_3$]BF$_4$ (160 mg, 0.21 mmol) in tetrahydrofuran (THF, 25 mL) was added dropwise a solution of NaSPh (35 mg, 0.27 mmol), also in THF (25 mL). The color of the combined solutions changed from colorless to light yellow. After stirring 1.5 h, solvent was removed under vacuum. The residue was extracted into toluene (30 mL), filtered and evaporated to yield a light-yellow amorphous powder, characterized as a mixture of species by ^{1}H NMR spectroscopy. The solids were redissolved in toluene and allowed to stand at room temperature, and a small quantity of colorless crystals was eventually obtained (ca. 10 mg, 0.01 mmol, 5% yield), and recovered by filtration. Anal. Calcd (found) for $C_{60}H_{60}B_2FeN_{12}O_2$, [(Tp^{Ph,Me})$_2$Fe]·$2H_2O$: C, 68.07 (68.07); H, 5.71 (5.49); N, 15.88 (15.92).

X-ray Crystallography. Diffraction-quality crystals of [Tpm^{Ph}Mn(NCMe)$_3$](BF$_4$)$_2$ (**2**^{Mn}), [Tpm^{Ph}Ni(NCMe)$_3$](BF$_4$)$_2$·NCMe (**2**^{Ni}·NCMe), [Tp^{Me,Me}Fe(NCMe)$_3$](BF$_4$)·^{1}/$_2$NCMe (**3**^{Fe}·^{1}/$_2$NCMe), [Tp^{Me,Me}Co(NCMe)$_3$](BF$_4$)·^{1}/$_2$NCMe (**3**^{Co}·^{1}/$_2$NCMe), and [Tp^{Ph,Me}Fe(NCMe)$_3$](BF$_4$)·^{1}/$_2$NCMe (**4**^{Fe}·^{1}/$_2$NCMe) were grown by vapor diffusion of diethyl ether into concentrated CH_3CN solutions. Crystals of [(Tp^{Ph,Me})$_2$Fe] were obtained from decomposition of [Tp^{Ph,Me}Fe−SPh] in toluene. Crystals of appropriate size were washed with perfluoropolyether PFO-XR75 and sealed under nitrogen in a glass capillary. Each sample was optically aligned on the four-circle of a Siemens P4 diffractometer equipped with a graphite monochromator, a monocap collimator, a Mo Kα radiation source (λ = 0.71073 Å), and a SMART CCD detector.[25] A semiempirical

dx.doi.org/10.1021/ic301409s | Inorg. Chem. 2012, 51, 12707−12719

Table 1. Summary of X-ray Crystallography

	$[Tpm^{Ph}Mn(NCMe)_3](BF_4)_2$ ($\mathbf{2}^{Mn}$)	$[Tpm^{Ph}Ni(NCMe)_3](BF_4)_2 \cdot NCMe$ ($\mathbf{2}^{Ni}\cdot NCMe$)	$[Tp^{Me,Me}Fe(NCMe)_3](BF_4)\cdot {}^1/_2NCMe$ ($\mathbf{3}^{Fe,1}/_2NCMe$)	$[Tp^{Me,Me}Co(NCMe)_3](BF_4)\cdot {}^1/_2NCMe$ ($\mathbf{3}^{Co,1}/_2NCMe$)	$Tp^{Ph,Me}Fe(NCMe)_3](BF_4)\cdot {}^1/_2NCMe$ ($\mathbf{4}^{Fe,1}/_2NCMe$)	$[(Tp^{Ph,Me})_2Fe]$
empirical formula	$C_{34}H_{31}B_2F_8MnN_9$	$C_{36}H_{34}B_2F_8N_{10}Ni$	$C_{22}H_{32.5}B_2F_4FeN_{9.5}$	$C_{22}H_{32.5}B_2CoF_4N_{9.5}$	$C_{37}H_{38.5}B_2F_4FeN_{9.5}$	$C_{60}H_{56}B_2FeN_{12}$
formula weight	794.24	839.06	583.55	586.63	769.74	1022.64
temperature (K)	293(2)	293(2)	293(2)	293(2)	293(2)	293(2)
crystal system	triclinic	monoclinic	hexagonal	hexagonal	triclinic	monoclinic
space group	$P\bar{1}$	$P2_1/n$	$R\bar{3}$	$R\bar{3}$	$P\bar{1}$	$C2/c$
a (Å)	12.6467(9)	12.3799(8)	11.6034(6)	11.6161(9)	11.5754(9)	18.410(2)
b (Å)	12.9873(9)	16.636(1)	11.6034(6)	11.6161(9)	12.2814(9)	13.826(2)
c (Å)	13.4015(9)	19.513(1)	37.890(3)	37.839(4)	15.408(1)	22.016(3)
α (deg)	67.315(1)	90	90	90	67.126(1)	90
β (deg)	70.336(1)	92.677(1)	90	90	77.677(1)	111.678(2)
γ (deg)	73.350(1)	90	120	120	76.193(1)	90
V (Å^3)	1881.1(2)	4014.3(4)	4418.0(4)	4421.7(7)	1942.0(3)	5207(1)
Z	2	4	6	6	2	4
density (calc, g/cm^3)	1.402	1.388	1.316	1.322	1.316	1.304
absorption coefficient (mm^{-1})	0.429	0.561	0.566	0.636	0.447	0.343
crystal color, morphology	amber fragment	purple fragment	light orange fragment	orange fragment	light green fragment	colorless block
crystal size (mm)	0.54 × 0.42 × 0.40	0.24 × 0.40 × 0.42	0.14 × 0.40 × 0.42	0.20 × 0.38 × 0.40	0.16 × 0.28 × 0.54	0.30 × 0.28 × 0.20
reflections collected	13066	27327	9721	10468	14016	18215
independent reflections (R_{int})	8270 (0.0340)	9148 (0.0448)	2248 (0.0378)	2260 (0.0610)	8709 (0.0339)	5923 (0.0532)
observed reflections	6823	7101	2048	1721	6734	3385
data/restraints/parameters	8270/74/546	9148/10/535	2248/0/115	2260/0/115	8709/22/549	5923/0/342
GOF	1.025	1.025	1.052	1.051	1.020	1.018
$R1$, $wR2$ [$I > 2\sigma(I)$]	0.0546, 0.1524	0.0545, 0.1545	0.0448, 0.1352	0.0470, 0.1385	0.0496, 0.1352	0.0466, 0.1136
$R1$, $wR2$ (all data)	0.0643, 0.1642	0.0700, 0.1703	0.0474, 0.1382	0.0630, 0.1478	0.0665, 0.1484	0.0972, 0.1351
difference peak, hole (e/Å^3)	0.355, −0.231	0.618, −0.366	0.563, −0.319	0.376, −0.339	0.567, −0.309	0.278, −0.225

dx.doi.org/10.1021/ic301409s | Inorg. Chem. 2012, 51, 12707−12719

Table 2. Bond Lengths and Angles

complex	2^{Mn}	2^{Ni}	3^{Fe}	3^{Co}	4^{Fe}	$[(Tp^{Ph,Me})_2Fe]$
M−Npz (Å)	2.307(2) [N1]	2.136(2) [N1]	2.142(1) [N1]	2.116(2) [N1]	2.150(2) [N1]	2.218(2) [N1]
	2.292(2) [N3]	2.139(2) [N3]			2.194(2) [N3]	2.270(2) [N3]
	2.291(2) [N5]	2.139(2) [N5]			2.190(2) [N5]	2.233(2) [N5]
M−NCMe (Å)	2.209(2) [N7]	2.063(2) [N7]	2.232(2) [N3]	2.182(2) [N3]	2.204(2) [N7]	
	2.217(2) [N8]	2.080(2) [N8]			2.190(2) [N8]	
	2.231(2) [N9]	2.075(3) [N9]			2.202(2) [N9]	
Npz−M−Npz, cis (deg)	80.77(6) [N1, N3]	86.06(8) [N1, N3]	88.45(5) [N1, N1′]	88.35(7) [N1, N1′]	88.50(7) [N1, N3]	90.57(7) [N1, N3]
	81.90(6) [N1, N5]	87.05(8) [N1, N5]			85.57(6) [N1, N5]	88.94(7) [N1, N5]
	80.32(6) [N3, N5]	84.72(8) [N3, N5]			90.32(6) [N3, N5]	88.26(7) [N3, N5]
						97.4(1)[a] [N1, N1′]
						83.73(7)[a] [N1, N3′]
						98.07(7)[a] [N3, N5′]
						85.9(1)[a] [N5, N5′]
MeCN−M−NCMe, cis (deg)	90.27(7) [N7, N8]	87.21(9) [N7, N8]	87.96(7) [N3,N3′]	87.75(9) [N3,N3′]	83.13(8) [N7, N8]	
	86.01(8) [N7, N9]	86.5(1) [N7, N9]			88.29(7) [N7, N9]	
	85.88(8) [N8, N9]	89.8(1) [N8, N9]			87.48(7) [N8, N9]	
Npz−M−NCMe, cis (deg)	88.65(7) [N1, N8]	87.73(8) [N1, N8]	92.26(6) [N1,N3′]	92.55(8) [N1,N3′]	91.31(7) [N1, N8]	
	101.55(7) [N1, N9]	96.85(9) [N1, N9]	91.33(6) [N1,N3″]	91.37(8) [N1,N3″]	97.85(7) [N1, N9]	
	100.64(7) [N3, N7]	99.08(8) [N3, N7]			97.46(8) [N3, N7]	
	93.12(7) [N3, N9]	89.50(9) [N3, N9]			88.83(7) [N3, N9]	
	90.81(7) [N5, N7]	90.18(9) [N5, N7]			88.41(7) [N5, N7]	
	101.42(7) [N5, N8]	96.44(9) [N5, N8]			93.41(7) [N5, N8]	
Npz−M−NCMe, trans (deg)	172.26(7) [N1, N7]	173.93(8) [N1, N7]	179.26(6) [N1,N3]	179.05(8) [N1,N3]	171.55(7) [N1, N7]	
	168.96(6) [N3, N8]	173.61(9) [N3, N8]			176.24(6) [N3, N8]	
	172.07(7) [N5, N9]	172.80(8) [N5, N9]			176.46(7) [N5, N9]	
Npz−M−Npz, trans (deg)						169.80(7)[a] [N1, N5′]
						171.4(1)[a] [N3, N3′]

[a]Interligand angle.

dx.doi.org/10.1021/ic301409s | Inorg. Chem. 2012, 51, 12707−12719

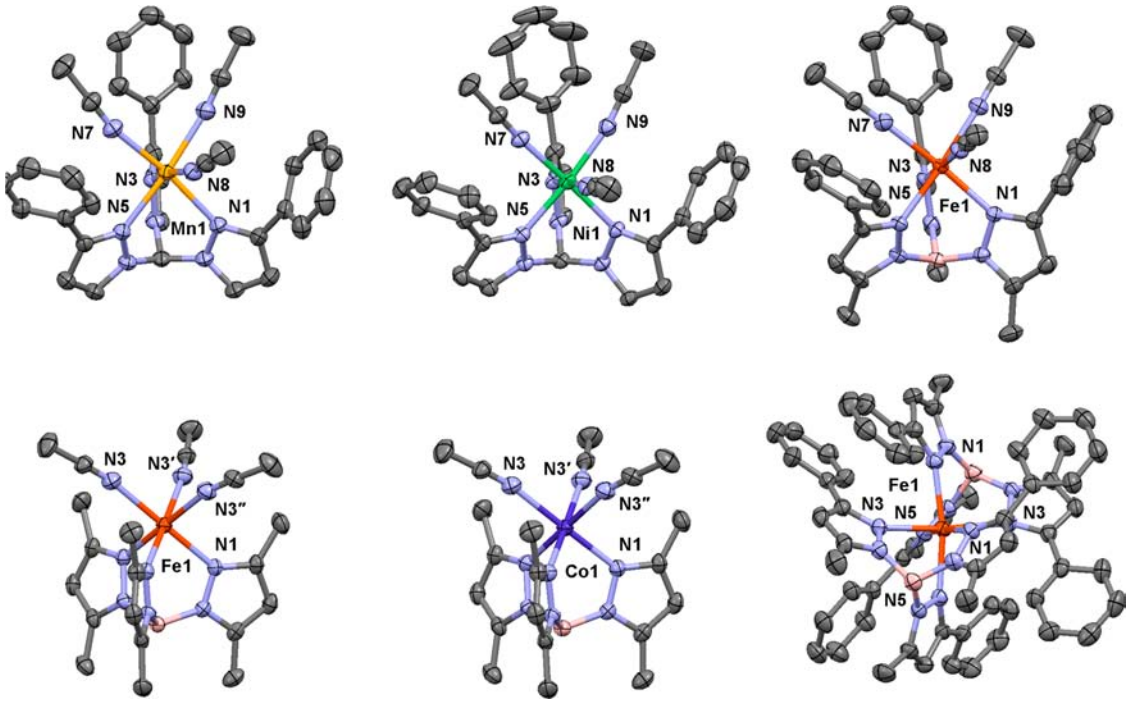

Figure 1. Thermal ellipsoid plots (30% probability) of the complex dications $\mathbf{2}^{Mn}$ (top left) and $\mathbf{2}^{Ni}$ (top center); the complex cations $\mathbf{4}^{Fe}$ (top right), $\mathbf{3}^{Fe}$ (bottom left), and $\mathbf{3}^{Co}$ (bottom center); and the neutral sandwich complex $[(Tp^{Ph,Me})_2Fe]$ (bottom right). Hydrogen atoms are omitted for clarity.

absorption correction was applied using the SADABS routine available in SAINT.[26,27] The data were corrected for Lorentz and polarization effects. The structures were solved by a combination of the Patterson heavy atom method and difference Fourier analysis with the use of SHELXTL 6.1.[28] Idealized positions for the hydrogen atoms were included as fixed contributions using a riding model with isotropic temperature factors set at 1.2 (B−H, methine and aromatic hydrogens) or 1.5 (methyl hydrogens) times that of the adjacent carbon atom. The positions of the methyl hydrogen atoms were optimized by a rigid rotating group refinement with idealized angles. Both anions in the structure of $\mathbf{2}^{Mn}$ exhibited two-site disorder (ca. 0.43:0.57 and 0.27:0.73) involving approximately 60° rotation about one B−F bond. The B−F bonds and the interatomic F···F separations were constrained to 1.35 ± 0.01 and 2.20 ± 0.01 Å, respectively, and the anisotropic ellipsoids for the F atoms were refined using the ISOR option. One anion was similarly disordered in the structure of $\mathbf{2}^{Ni}$·NCMe, and the lattice NCMe molecule was poorly resolved. The anion was refined using a two-site disorder model (ca. 0.81:0.19), with the B−F bonds and the interatomic F···F separations constrained to 1.35 ± 0.02 and 2.15 ± 0.01 Å, respectively; the F atoms of the major site were refined anisotropically. $\mathbf{2}^{Ni}$·NCMe is isomorphous to the previously reported iron and cobalt analogues.[18] $\mathbf{3}^{Fe}\cdot{}^1/_2$NCMe and $\mathbf{3}^{Co}\cdot{}^1/_2$NCMe are isomorphous; the free NCMe molecule present in both lattices was disordered over an inversion center and was treated as a diffuse electron density contribution with the aid of the SQUEEZE routine in the program PLATON.[29] In $\mathbf{4}^{Fe}\cdot{}^1/_2$NCMe, the anion exhibited two-site disorder (ca. 0.55:0.45), and the lattice NCMe molecule was disordered over an inversion center. The B−F bonds, interatomic F···F separations, C≡N and C−C bonds were constrained to 1.35, 2.10, 1.10, and 1.45 ± 0.01 Å, respectively. $[(Tp^{Ph,Me})_2Fe]$ is isomorphous with the cobalt and nickel analogues;[30,31] the iron atom sits on a 2-fold crystallographic axis, so only half of the molecule is unique.

Crystal and refinement data are summarized in Table 1. Relevant bond lengths and angles are listed in Table 2. Thermal ellipsoid plots are shown in Figure 1.[32]

3. RESULTS AND DISCUSSION

General Remarks. We prepared and characterized a series of scorpionate-supported half-sandwich complexes with acetonitrile coligands, $\mathbf{1}^{M}$−$\mathbf{4}^{M}$ (except $\mathbf{3}^{Mn}$, Scheme 1). Formation of sandwich complexes was discouraged by introducing 3-pyrazolyl ligand substituents, proximal to the metal center; nonetheless, the sandwich complex $[(Tp^{Me,Me})_2Mn]$[16] was inevitably formed instead of $[Tp^{Me,Me}Mn(NCMe)_3]BF_4$ ($\mathbf{3}^{Mn}$), while the other targeted product complexes were obtained successfully. The lone instance of sandwich formation likely results from the particular combination of the least bulky, most nucleophilic anionic tripodal ligand with the largest, most kinetically labile metal ion.[33] The product complexes were characterized by X-ray crystallography, and by ^{1}H NMR, electronic, and vibrational spectroscopy. The data support informative comparisons to the structures and spectra of both the sandwich complexes and the solvated metal complexes $[M^{II}(NCMe)_6]^{2+}$. A number of structural and spectroscopic trends were identified that provide quantitative insights into the effects of scorpionate ligand charge and sterics, as well as the identity of the metal itself, on the bonding within the complexes.

Compositional Analyses. Anomalous analytical data were obtained for the new complexes, which require explanation and investigation. Analytical data for the previously characterized sandwich complex $[(Tp^{Me,Me})_2Mn]$[16] obtained herein do correspond to the assigned formulation. Data for $\mathbf{2}^{Ni}$, $\mathbf{2}^{Mn}$, and $\mathbf{1}^{Mn}$ were also consistent with formulations given in the Experimental Section, allowing for the presence of about 1.0 equiv of adventitious H_2O, apparently introduced by brief exposure of the hygroscopic salts to atmosphere (since the crystal structure determinations of $\mathbf{2}^{Mn}$ and $\mathbf{2}^{Ni}$ did not show any H_2O in the lattices, vide supra). Analytical data for the other seven complex salts $\mathbf{3}^{M}$ and $\mathbf{4}^{M}$ were also consistent with

dx.doi.org/10.1021/ic301409s | Inorg. Chem. 2012, 51, 12707−12719

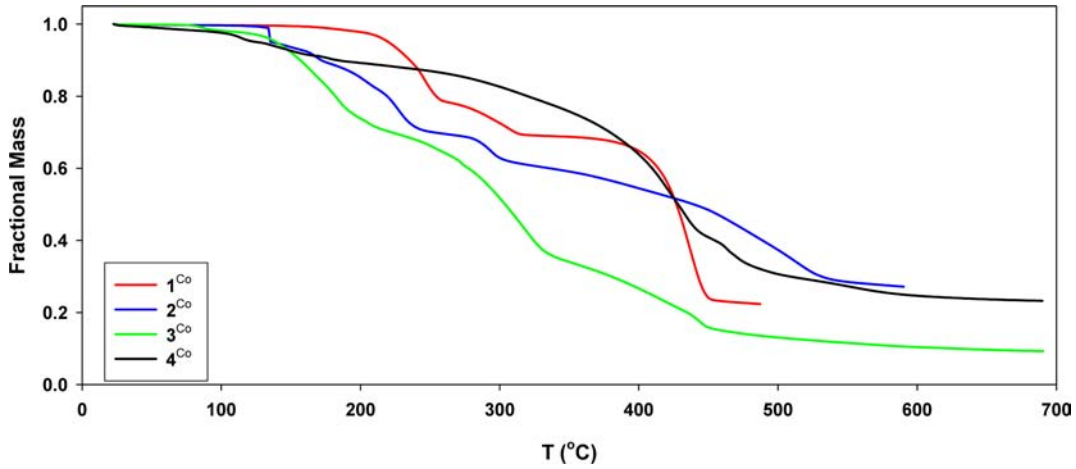

Figure 2. Thermogravimetric data for $\mathbf{1}^{Co}$–$\mathbf{4}^{Co}$.

introduction of 0.5–3.0 equiv of H_2O; moreover, their nitrogen analyses were consistently low, reflecting loss of multiple acetonitrile molecules (and excluding formation of sandwich complexes). Considering previously reported results for $\mathbf{1}^{Fe}$, $\mathbf{2}^{Fe}$ and $\mathbf{1}^{Co}$,[18] apparent loss of acetonitrile generally increased in severity with basicity of the scorpionate ligand, $\mathbf{2}^{M} < \mathbf{1}^{M} < \mathbf{4}^{M} < \mathbf{3}^{M}$; data for $\mathbf{3}^{Fe}$ and $\mathbf{3}^{Co}$ were consistent with complete loss of 3.5 equiv of bound and lattice acetonitrile molecules. Given the structural characterization of half-sandwich tris(aquo) scorpionate complexes analogous to $\mathbf{1}^{Fe}$ and $\mathbf{3}^{Ni}$,[34−37] the gain of H_2O and loss of CH_3CN may be coupled to some degree.

To offset ambiguity in the interpretation of analytical data, thermogravimetric analyses were conducted on crystalline samples of $\mathbf{1}^{Co}$–$\mathbf{4}^{Co}$ (Figure 2 and in Supporting Information, Figures S1–S4). The TGA traces for $\mathbf{1}^{Co}$ and $\mathbf{2}^{Co}$ were essentially identical to those previously reported.[18] Initial loss of mass from $\mathbf{1}^{Co}$ above about 150 °C was interpreted as dehydration of about 1.0 equiv of H_2O, followed by loss of three CH_3CN ligands between 200 and 250 °C, breakdown of a BF_4^- counterion near 300 °C, and loss of the $Tpm^{Me,Me}$ ligand above 350 °C (Supporting Information, Figure S1). For $\mathbf{2}^{Co}$, the TGA curve shifted to lower temperatures, initiated by loss of the lattice CH_3CN molecule observed by X-ray crystallography at 130 °C,[18] followed sequentially by dehydration of about 2.0 equiv of H_2O, loss of three CH_3CN ligands and complicated breakdown of the counterions and Tpm^{Ph} ligand (Supporting Information, Figure S2). The TGA curves of $\mathbf{3}^{Co}$ and $\mathbf{4}^{Co}$ exhibited comparable features (Supporting Information, Figures S3 and S4), but shifted to still lower temperatures, with mass loss observed for $\mathbf{4}^{Co}$ even at room temperature. In summary, given simple absorption of 0–2 equiv of H_2O upon exposure of the crystals to air, as well as the presence of lattice solvent confirmed by X-ray crystallography for $\mathbf{3}^{Co}$ herein (vide supra) and $\mathbf{2}^{Co}$ previously,[18] the TGA data are fully consistent with the formulations assigned to $\mathbf{1}^{Co}$–$\mathbf{4}^{Co}$, and demonstrate facile thermal loss of acetonitrile.

Further evidence for the loss of acetonitrile ligands was observed for hydrotris(pyrazolyl)borate complexes $\mathbf{3}^{M}$ and $\mathbf{4}^{M}$ (M = Co, Ni), as indicated by slow color changes in isolated crystalline solids under ambient conditions, from orange to violet (M = Co) or from blue to green (M = Ni). Decomposed solids derived from $\mathbf{3}^{M}$ were dissolved in noncoordinating CH_2Cl_2, and electronic spectra were consistent with pentacoordinate ligand fields (Supporting Information, Figures S5 and S6);[38,39] titrations with CH_3CN prompted significant restoration of the ligand field bands observed for the hexacoordinate complexes in neat CH_3CN (vide infra). The X-ray structure of green $[Tp^{Ph,Me}Ni(NCMe)_2](OTf)$, obtained by recrystallization of the blue triflate salt analogous to $\mathbf{4}^{Ni}$ from CH_2Cl_2/hexane, was previously reported.[19]

Magnetic Susceptibilities. Solution magnetic moments (μ_{eff}) in the ranges of 5.9, 5.3–5.9, 4.8–5.0, and 2.8–3.1 μ_B were determined by the Evans NMR method[24] in CD_3CN solutions for the Mn^{II}, Fe^{II}, Co^{II}, and Ni^{II} complexes, respectively (Supporting Information, Table S1). These values are consistent with high-spin ground states ($^6A_{1g}$, $^5T_{2g}$, $^4T_{1g}$, and $^3A_{2g}$ for Mn^{II}, Fe^{II}, Co^{II}, and Ni^{II}, respectively, in an ideal O_h ligand field),[33] and compare to the respective spin-only values (μ_S) of 5.92, 4.90, 3.87, and 2.83 μ_B for S = 5/2, 2, 3/2, 1. These high spin states, in which both dσ* orbitals (i.e., e_g under O_h symmetry) are singly occupied, induce the observed lability of the acetonitrile ligands.

Spin crossover was reported for related Fe^{II} sandwich complexes: $[(Tp^{Me,Me})_2Fe]$ is high-spin at room temperature,[40,41] but undergoes a gradual spin transition ($^5T_{2g} \leftrightarrow {}^1A_{1g}$) on cooling ($T_{1/2}$ = 195 K);[42] whereas $[(Tpm^{Me,Me})_2Fe]$ exhibits an abrupt transition coupled to a crystallographic phase change.[43] Therefore, we determined the temperature-dependent magnetic susceptibilities of $\mathbf{3}^{M}$ (M = Fe, Co) over a 5–300 K range. The data for $\mathbf{3}^{Fe}$ (Figure 3) fit the Curie–Weiss law (C = 3.60 emu-K/mol, θ = −1.4 K; μ_{eff} = 5.37 μ_B at 297 K) and are consistent with a high spin (S = 2) ground state; no spin crossover is observed. The data for $\mathbf{3}^{Co}$ (Supporting Information, Figure S7) show Curie–Weiss behavior above 150 K (C = 2.99 emu-K/mol; μ_{eff} = 4.89 μ_B), consistent with a high spin (S = 3/2) ground state. These results are comparable to solid-state data previously reported for $\mathbf{1}^{M}$ and $\mathbf{2}^{M}$ (M = Fe, Co),[18] and are consistent with pseudo-octahedral ligand fields.

X-ray Crystallography. Prior to this study, X-ray crystal structures were reported for $\mathbf{1}^{Fe}$, $\mathbf{1}^{Co}$, $\mathbf{2}^{Fe}$, and $\mathbf{2}^{Co}$ as tetrafluoroborate salts,[18] as well as $\mathbf{4}^{Co}$ and $\mathbf{4}^{Ni}$ as triflate salts.[19] Structures of complexes $\mathbf{2}^{Mn}$, $\mathbf{2}^{Ni}$, $\mathbf{3}^{Fe}$, $\mathbf{3}^{Co}$, and $\mathbf{4}^{Fe}$ were determined in the present work, as the tetrafluoroborate salts. Data for $\mathbf{1}^{Mn}$, $\mathbf{1}^{Ni}$, and $\mathbf{4}^{Mn}$ also confirmed the atom connectivity of these complexes (not shown), but disorder of the BF_4^- anion(s) and lattice solvent was intractable in each case. We did not obtain diffraction-quality crystals of $\mathbf{3}^{Ni}$. For comparative purposes, we also report the structure of the sandwich complex

dx.doi.org/10.1021/ic301409s | Inorg. Chem. 2012, 51, 12707–12719

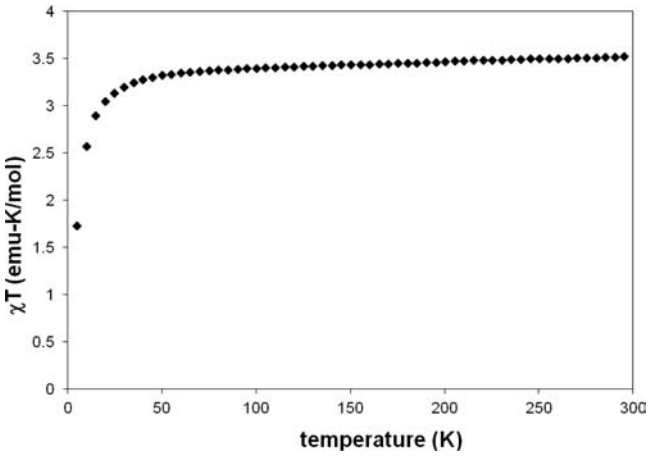

Figure 3. Temperature-dependent solid-state magnetic susceptibility of $\mathbf{3}^{Fe}$.

$[(Tp^{Ph,Me})_2Fe]$. Thermal ellipsoid plots are shown in Figure 1; relevant metal bond distances and angles are given in Table 2.

The complex (di)cations adopt a common piano-stool core structure with well-separated tetrafluoroborato counterion(s), and the metal center sandwiched between a κ^3-scorpionate and a facial array of three acetonitrile ligands, each *trans* to a nitrogen donor atom of the tripodal ligands. The complex cations of isomorphous $\mathbf{3}^{Fe}$ and $\mathbf{3}^{Co}$ occupy a crystallographic 3-fold axis, as previously observed for $\mathbf{1}^{Fe}$ and $\mathbf{1}^{Co}$, and the other structures also approach this ideal symmetry.

Average M−Npz and M−NCMe bond lengths of $\mathbf{2}^{Mn}$, $\mathbf{2}^{Ni}$, $\mathbf{3}^{Fe}$, $\mathbf{3}^{Co}$, and $\mathbf{4}^{Fe}$ can be compared (Supporting Information, Tables S2−S4)[44,45] with those of the previously reported half-sandwich analogues,[18,19] the sandwich complexes $[(Tpm^{Me,Me})_2M]$ (M = Fe,[43,46−51] Co,[52] Ni[52−55]), $[(Tp^{Me,Me})_2M]$ (M = Mn,[16] Fe,[40] Co,[56] Ni[57]), and the $[(Tp^{Ph,Me})_2Fe]$ sandwich complex reported herein and the Co^{II} and Ni^{II} analogues,[30,31] as well as the solvated cations $[M(NCMe)_6]^{2+}$ (M = Mn,[58] Fe,[59−62] Co,[63−67] Ni[67−71]). Of related interest are sandwich complexes of the hydrotris(1,2,4-triazol-1-yl)borato ligand, $[(Ttz^{Ph,Me})_2M]$ (M = Mn, Fe, Co, Ni, Cu, Zn).[72] The observed M−N bond lengths are uniformly consistent with high-spin electron configurations.[18,43,52,56,73]

For each class of compound, metal−ligand bond lengths decrease in the order Mn > Fe > Co > Ni (Figures 4, 5), consistent with the Irving−Williams series and the expected trends in nuclear charge, ionic radii, and crystal field stabilization energies.[74] The M−Npz bond lengths in the half-sandwich complexes (Supporting Information, Table S2) are generally shorter than in the sandwich complexes of the corresponding ligand (Supporting Information, Table S3).[30,31,40,43,46−57] In contrast, M−NCMe bond lengths in the half-sandwich complexes (Supporting Information, Table S2) are generally longer than in the corresponding solvated salts $[M(CNMe)_6]^{2+}$ (Supporting Information, Table S4).[58−71] This implies the tripodal scorpionate ligands are stronger donors than a facial triad of acetonitrile ligands, and a general observation in the half-sandwich complexes is an inverse relationship between the M−Npz and M−NCMe bond lengths for a given metal. However, this trend is modified by steric effects of the 3-pyrazole substituents as well as the scorpionate ligand charge.[18] M−Npz bond lengths in the half-sandwich complexes generally decrease in the order $\mathbf{2}^M > \mathbf{4}^M > \mathbf{1}^M > \mathbf{3}^M$, exhibiting a larger effect due to the 3-pyrazolyl substituent and

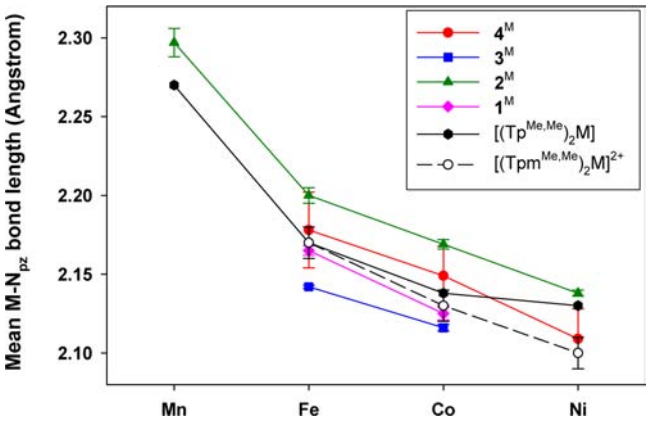

Figure 4. Plot of average M−N pyrazole bond lengths for $[(Tpm^{Me,Me})_2M]^{2+}$,[43,46−55] $[(Tp^{Me,Me})_2M]$,[16,40,56,57] and $\mathbf{1}^M$−$\mathbf{4}^M$.[18,19] Data are tabulated in Supporting Information, Tables S2, S4.

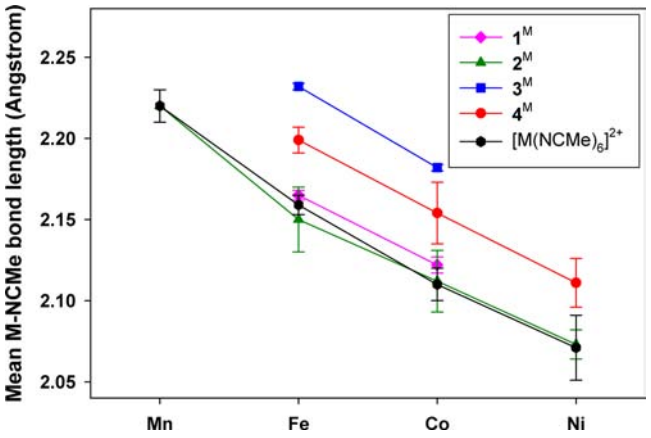

Figure 5. Plot of average M−NCMe bond lengths for $[M(NCMe)_6]^{2+}$,[58−71] and $\mathbf{1}^M$−$\mathbf{4}^M$.[18,19] Data are tabulated in Supporting Information, Tables S2, S4.

a smaller effect due to ligand charge. The M−NCMe bond distances generally increase in the order $\mathbf{2}^M < \mathbf{1}^M < \mathbf{4}^M < \mathbf{3}^M$, so the magnitude of these effects are reversed, and ligand charge is more important than sterics. These observations seem consistent with the analytical results; as discussed, the acetonitrile ligands are more readily displaced from the hydrotris(pyrazolyl)borate complexes. On the other hand, the M−Npz bonds are longer and the M−NCMe bonds are shorter in the tris(pyrazolyl)methane complexes. M−NCMe bond lengths are approximately equal in $\mathbf{2}^M$ and the solvated $[M(NCMe)_6]^{2+}$ complexes, indicating the bulky neutral Tpm^{Ph} ligand should exhibit a negligible chelate effect relative to solvation in dilute CH_3CN solution. Indeed, dissociations of $\mathbf{2}^M$ (M = Fe, Co, Ni) in such solutions were observed experimentally (vide infra).

The 3-pyrazole substituents also exert steric effects on the coordination geometry of the acetonitrile ligands. Superposition of the basal BN_3 atoms in experimental structures for the $Tp^{Me,Me}$-supported complex $\mathbf{3}^{Fe}$ and the $Tp^{Ph,Me}$-supported complex $\mathbf{4}^{Fe}$ indicates the facial array of solvent ligands is forced to rotate relative to the scorpionate tripod to accommodate the bulkier 3-phenyl substituents (Figure 6). The leading edge of a given phenyl ring pushes against one MeCN ligand, while the trailing MeCN ligand is pressed against the inner face of the ring. Moreover, the MeCN ligands of $\mathbf{3}^{Fe}$ are

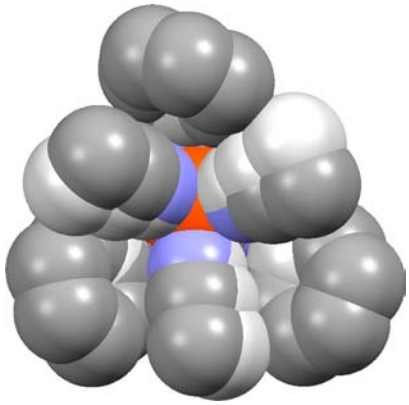

Figure 6. Space-filling diagram of a least-squares alignment (of basal BN_3 fragments) for the complex cations of $\mathbf{3}^{Fe}$ (gray) and $\mathbf{4}^{Fe}$ (color), emphasizing rotation of the facial tris(acetonitrile) ligand array enforced by the 3-phenyl pyrazole substituents on the latter. Hydrogen atoms omitted for clarity.

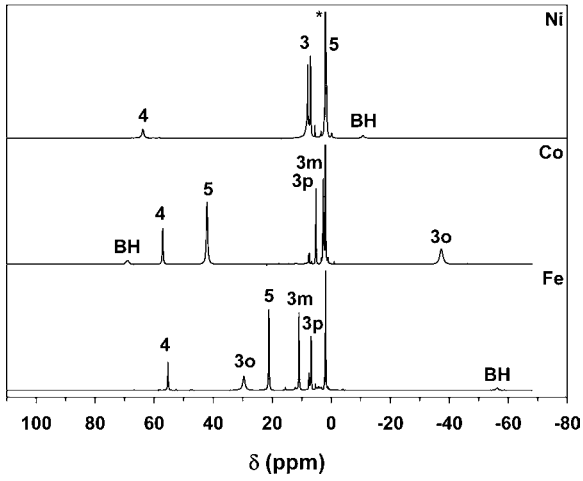

Figure 7. ^{1}H NMR spectra (CD_3CN, 295 K) of $\mathbf{4}^M$ (M = Ni, top; Co, middle; Fe, bottom). Peak marked (*) is due to free CH_3CN (1.96 ppm).

bent downward toward the $Tp^{Me,Me}$ ligand, with equivalent Fe−N≡C angles of 166.5(2)°, while the MeCN ligands of $\mathbf{4}^{Fe}$ bend upward and away from the $Tp^{Ph,Me}$ ligand, with the Fe−N≡C angles averaging 176.0(4)°. Inspection of analogous structural pairs indicates the bending and rotation of the facial acetonitrile triad are general phenomena.

In the complete structural series $\mathbf{2}^M$,[18] the nonbonded axial H−C···M distances also decrease with ionic radii, from 3.261(2) to 3.088(2) Å, in the expected order of Mn > Fe > Co > Ni. Even with exclusion of the uniquely large metal ion in $\mathbf{2}^{Mn}$, the chelate bites of the carbon-collared Tpm scorpionates are slightly more constrained than the boron-collared Tp analogues, with *cis* N_{pz}−M−N_{pz} bond angles averaging 85.1(5)° and 88.2(4)°, respectively. In contrast, the C−N−N−M torsion angles within the chelate arms correlate primarily with the 3-pyrazolyl substituents, averaging 9(1)° for $Tpm^{Me,Me}$- and $Tp^{Me,Me}$-supported complexes $\mathbf{1}^M$ and $\mathbf{3}^M$ (M = Fe, Co), and 16(2)° for the 3-phenyl analogues, $\mathbf{2}^M$ and $\mathbf{4}^M$ (M = Fe, Co).[18,19] Thus, the ligands exhibit some flexibility in accommodating metal ions and proximal ligand substituents of different sizes.

A similar steric effect is observed between 3-methyl substituents on opposing ligands of the sandwich complexes, which is diminished in the $[(Tpm^{Me,Me})_2M]^{2+}$ complexes relative to the $[(Tp^{Me,Me})_2M]$ analogues (Supporting Information, Table S3).[16,40,43,46−57] This leads to diverging M−Npz bond lengths over the series Fe < Co < Ni, with the values for $[(Tp^{Me,Me})_2M]$ departing from a parallel track relative to the half-sandwich complexes (Figure 4). Interligand steric contact is even more significant in the $[(Tp^{Ph,Me})_2M]$ sandwich complexes, which exhibit both longer and more dispersed M−Npz bond lengths (Supporting Information, Table S3).[30,31] For example, the $[(Tp^{Ph,Me})_2Fe]$ complex characterized herein (Figure 1) shows Fe−Npz bond lengths of 2.218(2)−2.270(2) Å (Table 2), compared to 2.196(2)−2.205(2) and 2.150(2)−2.194(2) Å in the half-sandwich complexes $\mathbf{2}^{Fe}$ and $\mathbf{4}^{Fe}$, respectively, and 2.147(4)−2.190(4) Å in $[(Tp^{Me,Me})_2Fe]$.[18,40]

NMR Spectroscopy. The complexes $\mathbf{1}^M$−$\mathbf{4}^M$ (M = Fe, Co, Ni) were characterized by ^{1}H NMR spectroscopy at room temperature (295 K) in CD_3CN solutions (Figure 7 and Supporting Information, Figures S8−S10). Given the typically slow electronic relaxation of high-spin Mn^{II} ($^6A_{1g}$ under ideal O_h symmetry) and the expected increase in NMR line-widths,[75,76] complexes $\mathbf{1}^{Mn}$, $\mathbf{2}^{Mn}$, and $\mathbf{4}^{Mn}$ were not examined. As anticipated for the other divalent metals with unpaired electrons, the observed resonances exhibit significant hyperfine shifts. Nonetheless, the complexes gave reasonably sharp, simple, and easily assigned spectra of four ($\mathbf{1}^M$, $\mathbf{3}^M$) or seven ($\mathbf{2}^M$, $\mathbf{4}^M$) expected ligand resonances, with equivalence of the pyrazolyl and 3-phenyl substituent rings reflecting effective C_{3v} symmetry. Assignments are listed for each complex in the Experimental Section, and are compared to those of the corresponding sandwich complexes in the Supporting Information, Table S5.[30,31,41,47,52,53,56,57,77,78]

Consistent with the orbitally nondegenerate ground state of Ni^{II} (ideally $^3A_{2g}$), large dipolar (through-space, pseudocontact) shifts are not expected for $\mathbf{1}^{Ni}$−$\mathbf{4}^{Ni}$, and the observed hyperfine shifts are dominated by through-bond contact shifts.[76,77,79] The aromatic 4-H pyrazolyl resonances of complexes $\mathbf{1}^{Ni}$−$\mathbf{4}^{Ni}$ and the 5-H pyrazolyl resonance of $\mathbf{3}^{Ni}$ exhibited significant downfield shifts, while the C/B−H, 3-Me and 5-Me pyrazolyl resonances were shifted somewhat upfield, and the 3-Ph pyrazolyl resonances remained close to the limiting diamagnetic shifts. The observed hyperfine shift patterns of $\mathbf{1}^{Ni}$, $\mathbf{3}^{Ni}$, and $\mathbf{4}^{Ni}$ were similar to those previously reported for the corresponding sandwich complexes,[31,53,57] but actual chemical shifts, particularly those of the 4-pyrazolyl resonances, were sufficiently different to distinguish the complexes (Supporting Information, Table S5).

Unlike Ni^{II}, the respective $^5T_{2g}$ and $^4T_{1g}$ ground states of the Fe^{II} and Co^{II} have partially occupied t_{2g} orbitals, giving rise to dipolar shifts; as previously shown for the sandwich complexes, the dipolar axis is aligned along the trigonal H−B/C···M vector, and the shifts exhibit both radial and azimuthal angular dependences (i.e., $[3\cos^2\theta - 1]/r^3$).[41,56,76−81] For the Co^{II} complexes, the methine ($\mathbf{1}^{Co}$ and $\mathbf{2}^{Co}$) or borohydride ($\mathbf{3}^{Co}$ and $\mathbf{4}^{Co}$) protons experience large downfield shifts relative to the Ni^{II} analogues, with the 5- and 4-pyrazolyl positions exhibiting progressively smaller dipolar shifting. In contrast, the 3-methyl substituents of $\mathbf{1}^{Co}$ and $\mathbf{3}^{Co}$ lie across the conical node, and the corresponding resonances are shifted well upfield, as are the *ortho* proton signals of the 3-phenyl substituents on $\mathbf{2}^{Co}$ and $\mathbf{4}^{Co}$. The signs of the dipolar shifts are reversed in the Fe^{II} complexes $\mathbf{1}^{Fe}$−$\mathbf{4}^{Fe}$ relative to the Co^{II} analogues, presumably reflecting changes in t_{2g} orbital splitting and occupancy.

dx.doi.org/10.1021/ic301409s | *Inorg. Chem.* 2012, 51, 12707−12719

Scheme 2

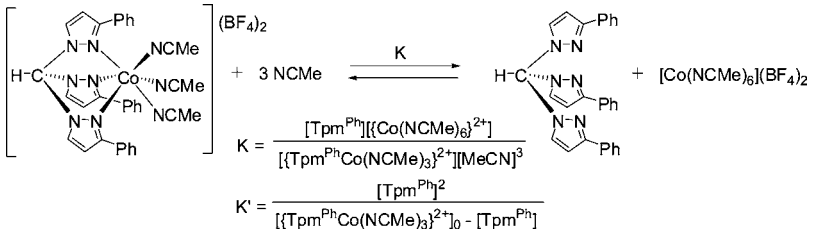

The ^{1}H NMR spectra of complexes $\mathbf{2}^{M}$ in CD_3CN all featured large diamagnetic resonances corresponding to the free Tpm^{Ph} ligand (Supporting Information, Figure S9). Thus, slow equilibria of $\mathbf{2}^{M}$ and the solvated complex ions $[M(NCMe)_6]^{2+}$ through reversible dissociation of the Tpm^{Ph} is indicated (Scheme 2). Neglecting temperature effects on CD_3CN density and activity, integration of the free ligand resonances against an internal ferrocene standard (9.6 mM) at four different and known concentrations of total added $\mathbf{2}^{Co}$ (16.5−34 mM) gave averaged values of the dissociation constant K' = 3.4(5)−5.8(7) mM over a temperature range 243−295 K, yielding ΔH^{o} = 1.4(1) kcal/mol, ΔS^{o} = −5.6(6) cal/molK (Figure 8). The

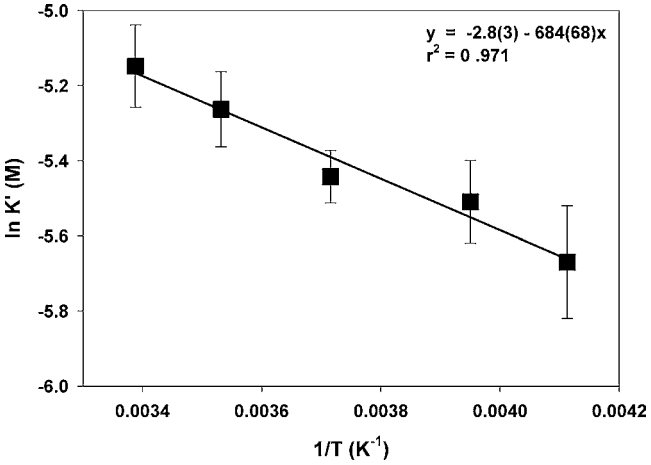

Figure 8. van't Hoff plot for equilibration of $\mathbf{2}^{Co}$ with free Tpm^{Ph} and $[Co(NCMe)_6](BF_4)_2$ in CD_3CN as determined by ^{1}H NMR spectroscopy against an internal ferrocene standard.

modest negative entropy may reflect differing degrees of solvent organization around the complex dications, as well as increased torsional rotation of pyrazole and phenyl rings in the displaced Tpm^{Ph} ligand.

Electronic Spectroscopy. UV−vis−NIR spectra of the complexes were obtained in acetonitrile solutions at room temperature (295 K). The C_{3v}-symmetric complexes exhibited electronic absorptions consistent with divalent transition metal ions in a weak ligand field under ideal octahedral symmetry.[33] Spectra of $\mathbf{3}^{M}$ (Fe, Co, Ni) are definitive of the class, and are shown in Figure 9. The remaining spectra are shown and summarized in the Supporting Information, Figures S11−S13, Table S6. As discussed in detail below, ligand field bands of the half-sandwich complexes are generally observed at energies intermediate between those reported for corresponding sandwich complexes and the solvated metal dications $[M(NCMe)_6]^{2+}$. As already described, the latter comprise a fraction of solutions derived from $\mathbf{2}^{M}$, and the respective spectra

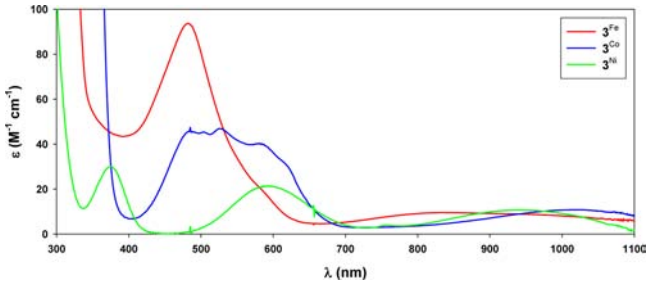

Figure 9. UV−vis−NIR spectra (CH_3CN, 295 K) of complexes $\mathbf{3}^{M}$ (M = Fe, Co, Ni).

are distinguished only by a tailing from the UV that arises from the Tpm^{Ph} ligand.

There are no spin-allowed ligand field transitions for high-spin Mn^{II} ($^6A_{1g}$).[33] Hence, the electronic spectra of complexes $\mathbf{1}^{Mn}$, $\mathbf{2}^{Mn}$, and $\mathbf{4}^{Mn}$ were completely featureless (Supporting Information, Figures S11−S13). Even the weak spin forbidden bands were obscured by tailing of strong UV absorption.

A single spin allowed band ($^5E_g \leftarrow {}^5T_{2g}$) is expected for high-spin Fe^{II} in the near-IR.[33] Spectra of the half-sandwich Fe(II) complexes each contain such a feature between 830 and 905 nm (i.e., Δ_O = 11,000−12,000 cm^{-1}), increasing in energy in the order $\mathbf{2}^{Fe} < \mathbf{1}^{Fe} < \mathbf{4}^{Fe} < \mathbf{3}^{Fe}$ (Figure 9 and Supporting Information, Figures S11−S13). In comparison, $[(Tp^{Me,Me})_2Fe]$ and $[Fe(NCMe)_6](BF_4)_2$ display bands at 800 nm (12,500 cm^{-1}, in $CHCl_3$)[41] and 910 nm (11,000 cm^{-1}),[82] respectively, bracketing the range just elucidated for the half-sandwich complexes. Because the ligand field bands appear in the near-IR, compounds $\mathbf{1}^{Fe}$ and $\mathbf{2}^{Fe}$ are pale yellow, and $\mathbf{4}^{Fe}$ is essentially colorless. In contrast, $\mathbf{3}^{Fe}$ exhibits a unique visible band at 478 nm (ε = 93 M^{-1} cm^{-1}), with a weak shoulder at 580 nm in acetonitrile solution (Figure 9). Assignment as a ligand field band of a low spin component is precluded by magnetic data. A strong charge transfer band of a trace ferric impurity is not excluded;[83−85] however, even the isolated crystals are pale orange in color. Alternatively, this band may be a weak LMCT transition arising from the $Tp^{Me,Me}$ ligand in $\mathbf{3}^{Fe}$.

The high-spin d^7 sandwich complex $[Tp_2Co]$ exhibits two relatively strong ligand field bands at 901 nm (11,100 cm^{-1}) and 459 nm (21,800 cm^{-1}), respectively assigned to $^4T_{2g}(F) \leftarrow {}^4T_{1g}(F)$ and $^4T_{1g}(P) \leftarrow {}^4T_{1g}(F)$ transitions; the third spin-allowed $^4A_{2g} \leftarrow {}^4T_{1g}(F)$ transition is a double excitation and is typically weak, while formally spin-forbidden transitions to several doublet states gain intensity through spin−orbit coupling.[76,86] Relative to this complex, the spin-allowed bands of $[Tpm_2Co]^{2+}$ are slightly blue-shifted (880 nm, 11,400 cm^{-1}; 450 nm, 22,200 cm^{-1}),[86,87] while $[(Tp^{Me,Me})_2Co]$ gives rise to a slightly red-shifted $^4T_{1g}(P) \leftarrow {}^4T_{1g}(F)$ band at 950 nm (10,500 cm^{-1}).[85] The corresponding bands of $[Co(NCMe)_6](BF_4)_2$

dx.doi.org/10.1021/ic301409s | Inorg. Chem. 2012, 51, 12707−12719

appear at 1017 nm (9800 cm^{-1}) and 476 nm (21,000 cm^{-1}), respectively.[82]

The half-sandwich complexes $\mathbf{1}^{Co}$–$\mathbf{4}^{Co}$ exhibit a $^4T_{2g}(F) \leftarrow {}^4T_{1g}(F)$ band between 970 and 1020 nm and a $^4T_{2g}(F) \leftarrow {}^4T_{1g}(F)$ band between 467 and 483 nm (Figure 9 and Supporting Information, Figures S11–S13), again at energies intermediate between those of the sandwich complexes and $[Co(NCMe)_6]^{2+}$. Compared to the other half-sandwich cobalt complexes (Supporting Information, Figures S11–S13), $\mathbf{3}^{Co}$ shows the most complicated and asymmetric visible band (Figure 9). Inspection of the average Co–Npz and Co–NCMe bond distances of $\mathbf{1}^{Co}$–$\mathbf{4}^{Co}$ indicates a relatively high degree of trigonal distortion in $\mathbf{3}^{Co}$ (Figures 4 and 5), which may generate unusual fine structure through term splitting or spin–orbit coupling of spin-forbidden bands. Alternatively, the ligand field bands may be convoluted with a feature akin to the anomalous visible band of $\mathbf{3}^{Fe}$.

Consistent with octahedral coordination of a d^8 ion,[33] the spectrum of $\mathbf{3}^{Ni}$ exhibits three spin-allowed bands (Figure 9), at 943 nm (10,600 cm^{-1}; $^3T_{2g} \leftarrow {}^3A_{2g}$), 597 nm (16,750 cm^{-1}; $^3T_{1g}(F) \leftarrow {}^3A_{2g}$) and 375 nm (26,700 cm^{-1}; $^3T_{1g}(P) \leftarrow {}^3A_{2g}$), as well as a weak spin-forbidden transition at 757 nm (13,200 cm^{-1}; $^1E_g \leftarrow {}^3A_{2g}$). $\mathbf{1}^{Ni}$, $\mathbf{2}^{Ni}$, and $\mathbf{4}^{Ni}$ all give similar spectra (Supporting Information, Figures S11–S13), although the $^3T_{1g}(P) \leftarrow {}^3A_{2g}$ transition at the highest energy is obscured by UV tailing in each case. The spectrum of $\mathbf{3}^{Ni}$ yields the ligand field parameters Δ_O = 10,600 cm^{-1} (B = 780 cm^{-1}), which can be compared to values for the sandwich complexes: $[Tp_2Ni]$, Δ_O = 11,800 cm^{-1} (B = 830 cm^{-1});[76] $[(Tp^{Me,Me})_2Ni]$, Δ_O = 11,400 cm^{-1};[85] and $[(Tpm^{Me,Me})_2Ni](BF_4)_2$, Δ_O = 11,700 cm^{-1} (B = 790 cm^{-1});[88] and for $[Ni(NCMe)_6]^{2+}$, Δ_O = 10,400 cm^{-1} (B = 890 cm^{-1}).[70,82]

FTIR Spectroscopy. All complexes were characterized by infrared spectroscopy in KBr matrixes (Figure 10, Supporting Information, Figures S14–S16 and Table S7). The $Tp^{R,Me}$ ligands of $\mathbf{3}^{M}$ (R = Me) and $\mathbf{4}^{M}$ (R = Ph) coordinate in tridentate fashion, consistent with the crystal structures (vide supra), as indicated by ν(B–H) absorptions in the range of 2523–2550 cm^{-1}.[89] The IR spectra of $\mathbf{1}^{M}$–$\mathbf{4}^{M}$ also show two diagnostic bands arising from the acetonitrile ligands, in distinct ranges of 2277–2298 cm^{-1} and 2303–2323 cm^{-1} that increase monotonically in the order Mn < Fe < Co < Ni. These energies are higher than the corresponding modes observed at 2252 cm^{-1} and 2293 cm^{-1} for free MeCN, which are ascribed to a Fermi resonance between the ν(C≡N) fundamental (ν_2) and a combination of ν(C–C) + $\delta(CH_3)$ modes ($\nu_3 + \nu_4$).[70,82] The nitrile lone pair has been assigned net σ^* character, so donation of electronic density to a metal ion would increase the frequency of ν(C≡N).[82] On the other hand, the various scorpionate ligands exert no discernible effect on the stretching frequencies, as indicated by nearly identical energies for two analogous bands observed for the octahedral metal salts, $[M^{II}(NCMe)_6]^{2+}$ (Supporting Information, Table S7).[17,58,63,66,70,82] The spectra of $\mathbf{2}^{Fe}$ and $\mathbf{3}^{M}$ are convoluted with features of a second species, presumably bis(acetonitrile) complexes arising from solvent ligand loss.[19]

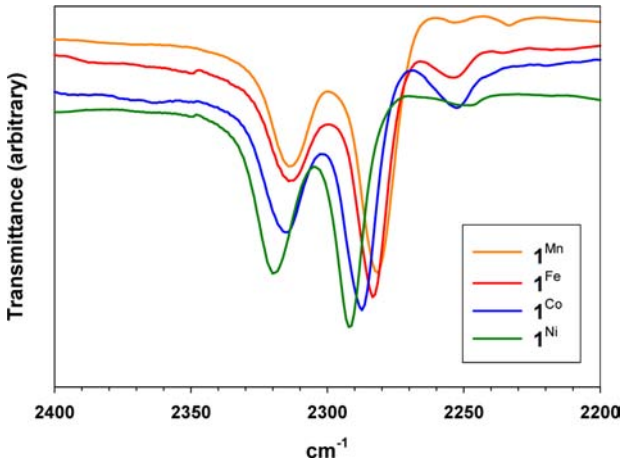

Figure 10. Detail of the FTIR spectra of $\mathbf{1}^{M}$ (KBr pellets: M = Mn, orange; Fe, red; Co, blue; Ni, green).

4. SUMMARY

Fifteen half-sandwich complexes $\mathbf{1}^{M}$–$\mathbf{4}^{M}$, except $\mathbf{3}^{Mn}$, were obtained by displacement of solvent ligands from $[M(NCMe)_x]^{2+}$ (M = Mn, x = 4; M = Fe, Co, Ni, x = 6) by addition of tripodal scorpionate ligands. The resulting half-sandwich complexes adopt high-spin electron configurations consistent with a weak ligand field. This leads to significant lability of the solvent ligands, particularly for the monocationic $Tp^{R,Me}$-supported complexes $\mathbf{3}^{M}$ (R = Me) and $\mathbf{4}^{M}$ (R = Ph) as well as the bulky, neutral Tpm^{Ph} ligand, which was observed to dissociate from its complexes $\mathbf{2}^{M}$ in acetonitrile solutions.

X-ray crystal structures of $\mathbf{2}^{Mn}$, $\mathbf{2}^{Ni}$, $\mathbf{3}^{Fe}$, $\mathbf{3}^{Co}$, and $\mathbf{4}^{Fe}$ are reported herein, as well as the bulky sandwich complex $[(Tp^{Ph,Me})_2Fe]$, and together with previously reported structures ($\mathbf{1}^{Fe}$, $\mathbf{1}^{Co}$, $\mathbf{2}^{Fe}$, $\mathbf{2}^{Co}$, $\mathbf{4}^{Co}$ and $\mathbf{4}^{Ni}$)[18,19] adopt a common piano stool geometry. The M–Npz and M–NCMe bond lengths show variations conforming to the Irving–Williams series, with significant secondary effects arising from scorpionate ligand sterics and charge. The structural trends reflect more qualitative observations of complex stability. For example, the M–NCMe bond lengths particularly depend on ligand charge, and the acetonitrile ligands are easily lost from monocationic complexes $\mathbf{3}^{M}$ and $\mathbf{4}^{M}$ of $[Tp^{R,Me}]^-$ ligands, while complexes of the bulky scorpionate ligands exhibit relatively long M–Npz bonds, and the neutral Tpm^{Ph} ligand is uniquely displaced from its complexes $\mathbf{2}^{M}$ in acetonitrile solutions. The steric bulk of a 3-phenyl pyrazole substituent also induces rotation of the facial tris(acetonitrile) ligand array relative to the methyl-substituted tripodal scorpionates, and influences M–N≡CMe bending angles.

The complexes were characterized by ^{1}H NMR, UV–vis–NIR, and FTIR spectroscopy. Numerous spectroscopic trends consistent with assigned geometric and electronic structures were elucidated, particularly with regard to ligand field parameters, which generally vary in the order sandwich > half-sandwich > $[M(NCMe)_6]^{2+}$, with more modest effects arising from the scorpionate ligands. Acetonitrile stretching modes also exhibited shifts reflecting σ donation to the various metal ions, which are nearly independent of the supporting coligands.

The labile half-sandwich complexes should prove useful as synthetic reagents and as catalyst precursors. The range of scorpionate ligand charge and sterics encompassed in the present work should enable systematic variation of reactivity. As we describe elsewhere,[15] these complexes were examined as nitrene transfer catalysts, extending previous reports of such reactivity for copper analogues.[7,8]

■ ASSOCIATED CONTENT

Supporting Information

Tabulation of structural and spectroscopic data (.pdf); X-ray crystallographic data (.cif). This material is available free of charge via the Internet at http://pubs.acs.org.

■ AUTHOR INFORMATION

Corresponding Author

*E-mail: jensenm@ohio.edu.

Notes

The authors declare no competing financial interest.

■ ACKNOWLEDGMENTS

The authors acknowledge the donors of the American Chemical Society Petroleum Research Fund (49296-DNI3) for support of this research. S.L. thanks the Condensed Matter and Surface Science program (CMSS) at Ohio University for a graduate research fellowship. We thank Professor Sunggyu Lee for access to his TGA instrument and Amber R. Tupper for technical assistance with the experiments.

■ REFERENCES

(1) Trofimenko, S. *J. Am. Chem. Soc.* **1967**, *89*, 3170−3177.
(2) Trofimenko, S. *Chem. Rev.* **1993**, *93*, 943−980.
(3) Pettinari, C. *Scorpionates II: Chelating Borate Ligands*; Imperial College Press: London, U.K., 2008.
(4) Trofimenko, S. *J. Am. Chem. Soc.* **1970**, *92*, 5118−5126.
(5) Pettinari, C.; Pettinari, R. *Coord. Chem. Rev.* **2005**, *249*, 525−543.
(6) Bigmore, H. R.; Lawrence, S. C.; Mountford, P.; Tredget, C. S. *Dalton Trans.* **2005**, 635−651.
(7) Diaz-Requejo, M. M.; Belderrain, T. R.; Nicasio, M. C.; Trofimenko, S.; Pérez, P. J. *J. Am. Chem. Soc.* **2003**, *125*, 12078−12079.
(8) Cano, I.; Nicasio, M. C.; Pérez, P. J. *Dalton Trans.* **2009**, 730−734.
(9) Brown, S. D.; Betley, T. A.; Peters, J. C. *J. Am. Chem. Soc.* **2003**, *125*, 322−323.
(10) Thomas, C. M.; Mankad, N. P.; Peters, J. C. *J. Am. Chem. Soc.* **2006**, *128*, 4956−4957.
(11) Nieto, I.; Ding, F.; Bontchev, R. P.; Wang, H.; Smith, J. M. *J. Am. Chem. Soc.* **2008**, *130*, 2716−2717.
(12) Cowley, R. E.; Bontchev, R. P.; Sorrell, J.; Sarracino, O.; Feng, Y.; Wang, H.; Smith, J. M. *J. Am. Chem. Soc.* **2007**, *129*, 2424−2425.
(13) Shay, D. T.; Yap, G. P. A.; Zakharov, L. N.; Rheingold, A. L.; Theopold, K. H. *Angew. Chem., Int. Ed.* **2005**, *44*, 1508−1510.
(14) Jenkins, D. M.; Betley, T. A.; Peters, J. C. *J. Am. Chem. Soc.* **2002**, *124*, 11238−11239.
(15) Liang, S.; Jensen, M. P. *Organometallics* **2012**, DOI: 10.1021/om3009102, in press.
(16) Xing, Y. H.; Aoki, K.; Bai, F. Y. *Synth. React. Inorg. Met.-Org. Chem.* **2004**, *34*, 1149−1163.
(17) Hathaway, B. J.; Holah, D. G.; Underhill, A. E. *J. Chem. Soc.* **1962**, 2444−2448.
(18) Edwards, P. G.; Harrison, A.; Newman, P. D.; Zhang, W. *Inorg. Chim. Acta* **2006**, *359*, 3549−3556.
(19) Uehara, K.; Hikichi, S.; Akita, M. *J. Chem. Soc., Dalton Trans.* **2002**, 3529−3538.
(20) Reger, D. L.; Grattan, T. C.; Brown, K. J.; Little, C. A.; Lamba, J. J. S.; Rheingold, A. L.; Sommer, R. D. *J. Organomet. Chem.* **2000**, *607*, 120−128.
(21) Wanke, R.; Smoleński, P.; da Silva, M. F. C. G.; Martins, L. M. D. R. S.; Pombeiro, A. J. L. *Inorg. Chem.* **2008**, *47*, 10158−10168.
(22) Chattopadhyay, S.; Deb, T.; Ma, H.; Petersen, J. L.; Young, V. G., Jr.; Jensen, M. P. *Inorg. Chem.* **2008**, *47*, 3384−3392.
(23) Gottlieb, H. E.; Kotlyar, V.; Nudelman, A. *J. Org. Chem.* **1997**, *62*, 7512−7515.
(24) Evans, D. F.; Jakubovic, D. A. *J. Chem. Soc., Dalton Trans.* **1988**, 2927−2933.
(25) *SMART*, V5.054; Bruker Analytical X-ray Systems: Madison, WI, 2001.
(26) *SAINT+*,V6.46; Bruker Analytical X-ray Systems: Madison, WI, 2003.
(27) Blessing, R. H. *Acta Crystallogr.* **1995**, *A51*, 33−38.
(28) *SHELXTL*, V6.14; Bruker Analytical X-ray Systems: Madison, WI, 2001.
(29) van der Sluis, P.; Spek, A. L. *Acta Crystallogr.* **1990**, *A46*, 194−201.
(30) Ruman, T.; Ciunik, Z.; Szklanny, E.; Wołowiec, S. *Polyhedron* **2002**, *21*, 2743−2753.
(31) Deb, T.; Rohde, G. T.; Young, V. G., Jr.; Jensen, M. P. *Inorg. Chem.* **2012**, *51*, 7257−7270.
(32) *Mercury*, 3.0; Cambridge Crystallographic Data Centre: Cambridge, U.K., 2012.
(33) Figgis, B. N. *Introduction to Ligand Fields*; Wiley: New York, 1966.
(34) López-Banet, L.; Santana, M. D.; García, G.; Pérez, J.; García, L.; Lezama, L.; Liu, M. *Polyhedron* **2012**, *31*, 575−586.
(35) Nakazawa, J.; Ogiwara, H.; Kashiwazaki, Y.; Ishii, A.; Imamura, N.; Samejima, Y.; Hikichi, S. *Inorg. Chem.* **2011**, *50*, 9933−9935.
(36) Hammes, B. S.; Carrano, M. W.; Carrano, C. J. *J. Chem. Soc., Dalton Trans.* **2001**, 1448−1451.
(37) Reger, D. L.; Little, C. A.; Rheingold, A. L.; Sommer, R.; Long, G. J. *Inorg. Chim. Acta* **2001**, *316*, 65−70.
(38) Banci, L.; Bencini, A.; Benelli, C.; Gatteschi, D.; Zanchini, C. *Struct. Bonding (Berlin)* **1982**, *52*, 37−86.
(39) Ma, H.; Chattopadhyay, S.; Petersen, J. L.; Jensen, M. P. *Inorg. Chem.* **2008**, *47*, 7966−7968.
(40) Oliver, J. D.; Mullica, D. F.; Hutchinson, B. B.; Milligan, W. O. *Inorg. Chem.* **1980**, *19*, 165−169.
(41) Jesson, J. P.; Trofimenko, S.; Eaton, D. R. *J. Am. Chem. Soc.* **1967**, *89*, 3158−3164.
(42) Jesson, J. P.; Weiher, J. F.; Trofimenko, S. *J. Chem. Phys.* **1968**, *48*, 2058−2066.
(43) Reger, D. L.; Little, C. A.; Young, V. G., Jr.; Pink, M. *Inorg. Chem.* **2001**, *40*, 2870−2874.
(44) Allen, F. H. *Acta Crystallogr.* **2002**, *B58*, 380−388.
(45) *ConQuest*, 1.14; Cambridge Crystallographic Data Centre: Cambridge, U.K., 2012.
(46) Reger, D. L.; Little, C. A.; Rheingold, A. L.; Lam, M.; Concolino, T.; Mohan, A.; Long, G. J. *Inorg. Chem.* **2000**, *39*, 4674−4675.
(47) Reger, D. L.; Little, C. A.; Rheingold, A. L.; Lam, M.; Liable-Sands, L. M.; Rhagitan, B.; Concolino, T.; Mohan, A.; Long, G. J.; Briois, V.; Grandjean, F. *Inorg. Chem.* **2001**, *40*, 1508−1520.
(48) A, L.-t.; Duan, L.-m.; Xu, X.-t.; Liu, S.-q. *Chem. Res. Chin. Univ.* **2009**, *25*, 273−278.
(49) Reger, D. L.; Little, C. A.; Smith, M. D.; Rheingold, A. L.; Lam, K.-C.; Concolino, T. L.; Long, G. J.; Hermann, R. P.; Grandjean, F. *Eur. J. Inorg. Chem.* **2002**, 1190−1197.
(50) Reger, D. L.; Smith, M. D.; Brown, K. J. *J. Chem. Crystallogr.* **2009**, *39*, 545−548.
(51) Lavrenova, L. G.; Virovets, A. V.; Peresypkina, E. V.; Strekalova, A. D.; Piryazev, D. A.; Daletsky, V. A.; Sheludyakova, L. A.; Vasilevsky, S. F. *Inorg. Chim. Acta* **2012**, *382*, 1−5.
(52) Reger, D. L.; Little, C. A.; Smith, M. D. *Inorg. Chem.* **2002**, *41*, 4453−4460.
(53) Michaud, A.; Fontaine, F.-G.; Zargarian, D. *Acta Crystallogr.* **2005**, *E61*, m784−m786.
(54) Michaud, A.; Fontaine, F.-G.; Zargarian, D. *Acta Crystallogr.* **2005**, *E61*, m904−m906.
(55) Liang, S.; Chattopadhyay, S.; Petersen, J. L.; Young, V. G., Jr.; Jensen, M. P. *Polyhedron* **2013**, in press, DOI: 10.1016/j.poly.2012.10.034.
(56) Myers, W. K.; Duesler, E. N.; Tierney, D. L. *Inorg. Chem.* **2008**, *47*, 6701−6710.

(57) Santana, M. D.; López-Banet, L.; García, G.; García, L.; Pérez, J.; Liu, M. *Eur. J. Inorg. Chem.* **2008**, 4012−4018.
(58) Weller, F.; Mai, H.-J.; Dehnicke, K. *Z. Naturforsch., B: Chem. Sci.* **1996**, *51*, 298−300.
(59) Brennessel, W. W.; Brooks, N. R.; Mehn, M. P.; Que, L., Jr.; Young, V. G., Jr. *Acta Crystallogr.* **2001**, *E57*, m545−m546.
(60) Kuhn, N.; Kotowski, H.; Maichle-Mößmer, C.; Abram, U. *Z. Anorg. Allg. Chem.* **1998**, *624*, 1653−1656.
(61) Constant, G.; Daran, J.-C.; Jeannin, Y. *J. Organomet. Chem.* **1972**, *44*, 353−363.
(62) Lavrentiev, I. P.; Korableva, L. G.; Lavrentieva, E. A.; Nifontova, G. A.; Khidekel, M. L.; Gusakovskaya, I. G.; Larkina, T. I.; Arutyunian, L. D.; Filipenko, O. S.; Ponomarev, V. I.; Atovmyan, L. O. *Transition Met. Chem.* **1980**, *5*, 193−200.
(63) Leigh, G. J.; Sanders, J. R.; Hitchcock, P. B.; Fernandes, J. S.; Togrou, M. *Inorg. Chim. Acta* **2002**, *330*, 197−212.
(64) Cotton, F. A.; Daniels, L. M.; Jordan, G. T., IV; Murillo, C. A. *Polyhedron* **1998**, *17*, 589−597.
(65) Malkov, A. E.; Fomina, I. G.; Sidorov, A. A.; Aleksandrov, G. G.; Egorov, I. M.; Latosh, N. I.; Chupakhin, O. N.; Rusinov, G. L.; Rakitin, Yu. V.; Novotortsev, V. M.; Ikorskii, V. N.; Eremenko, I. L.; Moiseev, I. I. *J. Mol. Struct.* **2003**, *656*, 207−224.
(66) Hijazi, A. K.; Al Hmaideen, A.; Syukri, S.; Radhakrishnan, N.; Herdtweck, E.; Voit, B.; Kühn, F. E. *Eur. J. Inorg. Chem.* **2008**, 2892−2898.
(67) Veith, M.; Gödicke, B.; Huch, V. *Z. Anorg. Allg. Chem.* **1989**, *579*, 99−110.
(68) Søtofte, I.; Hazell, R. G.; Rasmussen, S. E. *Acta Crystallogr.* **1976**, *B32*, 1692−1696.
(69) Leban, I.; Gantar, D.; Frlec, B.; Russell, D. R.; Holloway, J. H. *Acta Crystallogr.* **1987**, *C43*, 1888−1890.
(70) Bougon, R.; Charpin, P.; Christe, K. O.; Isabey, J.; Lance, M.; Nierlich, M.; Vigner, J.; Wilson, W. W. *Inorg. Chem.* **1988**, *27*, 1389−1393.
(71) Pietikäinen, J.; Maaninen, A.; Laitinen, R. S.; Oilunkaniemi, R.; Valkonen, J. *Polyhedron* **2002**, *21*, 1089−1095.
(72) Oseback, S. N.; Shim, S. W.; Kumar, M.; Greer, S. M.; Gardner, S. R.; Lemar, K. M.; DeGregory, P. R.; Papish, E. T.; Tierney, D. L.; Zeller, M.; Yap, G. P. A. *Dalton Trans.* **2012**, *41*, 2774−2787.
(73) Eichhorn, D. M.; Armstrong, W. H. *Inorg. Chem.* **1990**, *29*, 3607−3612.
(74) Gorelsky, S. I.; Basumallick, L.; Vura-Weis, J.; Sarangi, R.; Hodgson, K. O.; Hedman, B.; Fujisawa, K.; Solomon, E. I. *Inorg. Chem.* **2005**, *44*, 4947−4960.
(75) Bertini, I.; Luchinat, C. Nuclear Magnetic Resonance of Paramagnetic Substances in Solution. In *Physical Methods for Chemists*, 2nd ed; Drago, R. S., Ed.; Saunders: Fort Worth, TX, 1992; Chapter 12.
(76) Jesson, J. P.; Trofimenko, S.; Eaton, D. R. *J. Am. Chem. Soc.* **1967**, *89*, 3148−3158.
(77) Jesson, J. P. *J. Chem. Phys.* **1967**, *47*, 582−591.
(78) Aubagnac, J.-L.; Claramunt, R. M.; Elguero, J.; Gilles, I.; Sanz, D.; Trofimenko, S.; Virgili, A. *Bull. Soc. Chim. Belg.* **1995**, *104*, 473−482.
(79) Horrocks, W. D., Jr.; Taylor, R. C.; LaMar, G. N. *J. Am. Chem. Soc.* **1964**, *86*, 3031−3038.
(80) McGarvey, B. R. *J. Chem. Phys.* **1970**, *53*, 86−91.
(81) Długopolska, K.; Ruman, T.; Danilczuk, M.; Pogocki, D. *Appl. Magn. Reson.* **2008**, *35*, 271−283.
(82) Buschmann, W. E.; Miller, J. S. *Chem.—Eur. J.* **1998**, *4*, 1731−1737.
(83) Zamponi, S.; Gambini, G.; Conti, P.; Gioia Lobbia, G.; Marassi, R.; Berrettoni, M.; Cecchi, P. *Polyhedron* **1995**, *14*, 1929−1935.
(84) Mason, S. J.; Hill, C. M.; Murphy, V. J.; O'Hare, D.; Watkin, D. J. *J. Organomet. Chem.* **1995**, *485*, 165−171.
(85) De Alwis, D. C. L.; Schultz, F. A. *Inorg. Chem.* **2003**, *42*, 3616−3622.
(86) Jesson, J. P. *J. Chem. Phys.* **1966**, *45*, 1049−1056.
(87) Astley, T.; Gulbis, J. M.; Hitchman, M. A.; Tiekink, E. R. T. *J. Chem. Soc., Dalton Trans.* **1993**, 509−515.
(88) Nolet, M.-C.; Michaud, A.; Bain, C.; Zargarian, D.; Reber, C. *Photochem. Photobiol.* **2006**, *82*, 57−63.
(89) Northcutt, T. O.; Lachicotte, R. J.; Jones, W. D. *Organometallics* **1998**, *17*, 5148−5152.